QUANTIFICATION OF AMINE LOSS IN THE POST COMBUSTION CO_2 CAPTURE PROCESS

A Thesis

Submitted to the Faculty of Graduate Studies and Research

In Partial Fulfillment of the Requirements

for the Degree of

Master of Applied Science

In Environmental Systems Engineering

University of Regina

By

Amrutha Raghu

Regina, Saskatchewan

December, 2012

Copyright 2012: Amrutha Raghu

UNIVERSITY OF REGINA

FACULTY OF GRADUATE STUDIES AND RESEARCH

SUPERVISORY AND EXAMINING COMMITTEE

Amrutha Raghu, candidate for the degree of Master of Applied Science in Environmental Systems Engineering**,** has presented a thesis titled, ***Quantification of Amine Loss in the Post Combustion CO_2 Capture Process,*** in an oral examination held on November 16, 2012. The following committee members have found the thesis acceptable in form and content, and that the candidate demonstrated satisfactory knowledge of the subject material.

External Examiner:	Dr. David deMontigny, Process Systems Engineering
Supervisor:	Dr. Amornvadee Veawab, Environmental Systems Engineering
Committee Member:	Dr. Stephanie Young, Environmental Systems Engineering
Committee Member:	Dr. Adisorn Aroonwilas, Industrial Systems Engineering
Chair of Defense:	Dr. Nader Mobed, Department of Physics

*Not present at defense

ABSTRACT

During the process of CO_2 capture using amine solvents, there is a certain amount of solvent loss. Amine vapourization has been categorized under such solvent losses. A systematic approach is required to determine such losses. This study aims at quantifying amine vapourization loss for current operating plant conditions by an in-house process model using excel. Experimental data was generated for a binary solution of monoethanolamine (MEA) + water (H_2O) in a range of 1-7 kmol/m^3 at 80^oC using a Swietoslawski Ebulliometer. At this low concentration range of MEA, the correlation between activity coefficient and the concentration of MEA obtained was scattered. An empirical equation using Raoult's Law was developed as a function of the activity coefficient, concentration of amine, and temperature. The regressed data, for activity coefficient increased as a function of amine concentration, and saturated vapour pressure increased as a function of temperature. The amine loss from the top of the absorber corresponding to the amine plant conditions was studied using the derived empirical regressed equation. This study was based on the assumption that no cooling equipment being installed on the top of the absorber to reduce the escape of amine solvent with the treated gas. The parametric effects on amine loss in the gas absorption column were evaluated. The behaviour of lean CO_2 loading, feed gas temperature, concentration of amine, and the scrubbing process showed to have an effect on the loss due to vapourization.

ACKNOWLEDGEMENTS

I would like to sincerely thank my professor Dr. Amornvadee Veawab for her constant support and encouragement throughout this study. Her guidance and meticulous care have paved the way for me to complete this work. I would also like to thank Dr. Adisorn Aroonwilas who has played a major role in helping me with my research. He has been a great mentor and has constantly motivated me during this study. I would like to acknowledge the Faculty of Graduate Studies and Research at the University of Regina and the Natural Sciences and Engineering Research Council of Canada (NSERC) for providing financial support.

I would also like to extend my gratitude to all my friends for making this journey a delightful one. Last but not least, I would like to express my respect and love for my parents, sister, and brother, and for their prayers and blessings, which have been a driving force for every new day.

TABLE OF CONTENTS

LIST OF TABLES

LIST OF FIGURES

NOMENCLATURE

AMP	2-amino-2-methyl-1-propanol
a_b	Activity of substance b in the mixture
CCS	Carbon capture and storage
DEA	Diethanolamine
f_i	Fugacity of component i in the vapour phase
HEX	Heat exchanger
MEA	Monoethanolamine
MDEA	Methyldiethanolamine
mmscf	million standard cubic feet
NRTL	Non-Random Two Liquid
NOx	Nitrogen oxide compounds
PIPA	Piperazine
PAN	Polyacrylonitrile
psia	Per square inch absolute
p_i^{sat},p_i^*, P^s	Saturated vapour pressure
UNIQUAC	Universal Quasichemical
VOCs	Volatile organic compounds
VLE	Vapour liquid equilibrium
x_i	Mole fraction of component i in the liquid phase
y_i	Mole fraction of component i in the vapour phase

Greek letters

α	CO_2 loading
η	Efficiency
ϕ_i	Correction factor for individual parametric effect
μ_i	Partial molar Gibbs energy
μ_i^0	Chemical potential of the pure solvent *i* in the solution
ψ_{MEA}	MEA vapourization in a unit of kg/ton CO_2 captured
ψ_{base}	Base value of vapourization
γ_i	Activity coefficient of component i

1. INTRODUCTION

1.1 Absorption based CO_2 capture

Climate change is one of the main environmental problems. The main constituent of this problem is the emission of carbon dioxide (CO_2) into the atmosphere (Chowdhury et al., 2011). Anthropogenic activities, such as the burning of fossil fuels, are the foremost sources of CO_2 emissions. Various scientific approaches have been proposed and implemented to limit the emission of CO_2. Among those approaches, carbon capture and storage (CCS) is widely accepted as it can help reduce and stabilize the emission of CO_2 into the atmosphere (Kentish et al., 2008).

CCS involves the application of post-combustion capture, pre-combustion capture, and the oxy-fuel process (IPCC, 1990). Post combustion capture removes CO_2 from a stream of flue gas that is produced by fossil fuel combustion and contains up to 15% by volume of CO_2 (EIA, 2005). A number of gas separation technologies are technically viable; however, gas absorption into chemical solvents is the most promising among these processes (Cummings et al., 2008). In the pre-combustion process, the fuel is processed with steam and air to produce carbon-monoxide (CO) and hydrogen (H_2). Further treatment with steam produces H_2 and 15-60% by volume CO_2. CO_2 is removed from the gas stream by using a chemical or physical absorption processes resulting in H_2. The oxy-fuel process uses oxygen (O_2) instead of air to produce flue gas that is mainly water-vapour and 80% by volume CO_2 (Ciferno et al., 2009). The concentrated stream of CO_2 is further separated using techniques such as the use of a membrane, adsorption onto a solid sorbent, and cryogenic methods. Post combustion capture has the advantage of

being capable of being retro-fit with existing power plants, thus making it a feasible and mature process in CO_2 capture. Figure 1.1 exemplifies a post-combustion CO_2 capture process using amine-based absorption technology. The flue gas, which contains 10-15% CO_2, is introduced into the bottom of the absorber and flow's upward, against the current of the CO_2 lean amine solution fed into the top of the absorber. The absorber is operated at 40-60^{o}C, near atmospheric pressure, and the CO_2 from the flue gas is absorbed into the lean amine solution. The treated gas, which contains much less CO_2 content, leaves the absorber top to the atmosphere while the CO_2 rich amine solution leaves the absorber bottom to the rich lean heat exchanger. Typically, a water wash with a cooler is installed at the absorber top to minimize the carryover of amine solution with the treated gas caused by solution vapourization.

The CO_2 rich amine solution is heated by the CO_2 lean amine solution at the rich lean heat exchanger and then fed to the top of the regenerator for the desorption of CO_2. During the CO_2 desorption, the CO_2 rich amine solution is heated to 100-140^{o}C by a hot gaseous mixture of water vapour, amine, and CO_2 that is produced from a re-boiler. The stripped CO_2 exits the regeneration top with a certain amount of water vapour, which is recovered in the overhead condenser and recycled to the regenerator. The CO_2 lean amine solution leaves the regenerator and is fed into the rich lean heat exchanger to provide heat to the CO_2 rich amine solution. The CO_2 lean amine solution is further cooled before entering the absorber for reuse. The commonly used amines for this process, particularly for acid gas treatment, are monoethanolamine (MEA), diethanolamine (DEA),2-amino-2-methyl-1-propanol (AMP), methyldiethanolamine (MDEA), and piperazine (PIPA), (Puxty et al., 2009). An aqueous solution of blended amines has also been used.

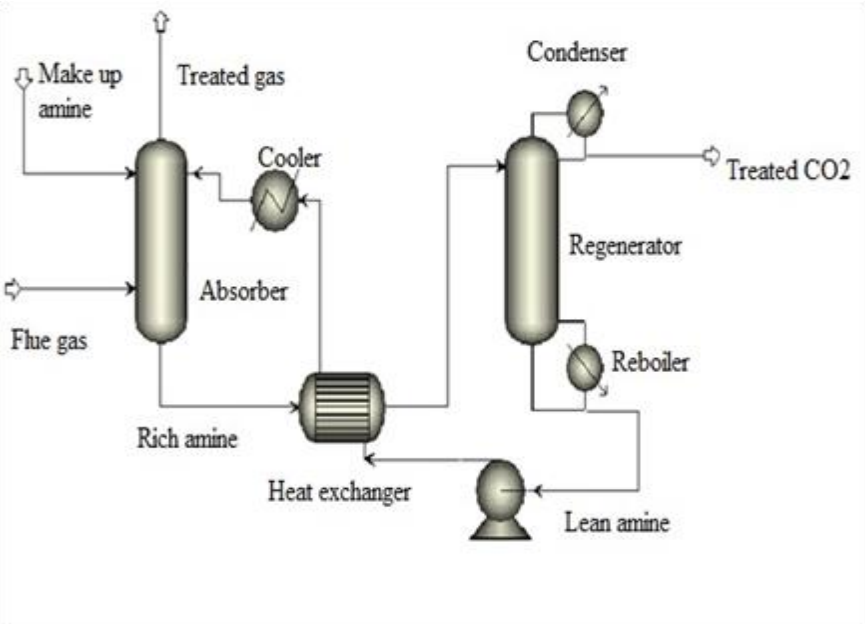

Figure 1.1: A simplified process flow diagram of the amine–based CO_2 capture process (Redrawn from Kohl & Neilson, 1997)

The tailoring of these blended amines enables an increase in gas absorption capacity rate and a reduction in energy consumption (Vrachnos et al., 2006).

1.2 Loss of absorption solvent

During the operation of the CO_2 capture process, the amine is gradually reduced due to several causes, including the entrainment of gas out of the absorber and regenerator, the vapourization of amine, and the degradation of amine. The reduction of amine concentration is commonly known as amine loss. Details of these types of amine loss are discussed below.

1.2.1 Entrainment loss

The amine loss due to gaseous entrainment occurs when the amine solution is carried away in the form of small droplets along with the gas stream. Entrainment can be described as spray or mist in liquid gas dispersion. It occurs when the amine solvent encounters high velocity of gas streams and gets entrapped in the gas stream that flows out of the absorber or the regenerator. Loss due to entrainment is attributed to the hydraulics of liquid and gas in the absorber or regenerator. Maintaining the velocity of gas flow helps in controlling the entrainment loss (Stewart and Lanning, 1994).

1.2.2 Vapourization loss

McLees (2006) defined vapourization loss as the process by which compounds escape from liquid phase to gas phase. It is said to be a direct result of vapour pressure of

amine solutions on the gas stream. The important parameters that contribute to the vapourization loss are temperature, pressure, and concentration of amine. These parameters maintain equilibrium between the vapour pressure of amine solution and the partial pressure of gas stream. As the temperature increases or pressure decreases, more amine from the solution tends to escape to the vapour phase to maintain equilibrium as treated gas is continuously being replaced by new gas stream. The loss is predominant in the absorber, regenerator, and the flash tank (Stewart and Lanning, 1994). An example of amine loss was reported for a 420 MW natural gas power plant emitting 1.2 million tonnes of CO_2 with constant functioning of the plant. It is estimated that with using amine absorption, 85% of the CO_2 could be captured and an amine emission of 40-160 tonnes is expected every year. The exact emission depends on the size of the power plant (Shao and Stangeland, 2009).

1.2.3 Amine degradation loss

During the removal of acid gases, prolonged use of amine leads to the formation of undesirable products from which amines are not easily recovered. This process of amine degradation causes amine loss and operational problems such as foaming, corrosion, high solution viscosity, and fouling, thereby decreasing the plant life. The three main degradation mechanisms in CO_2 capture are oxidative, thermal, and atmospheric degradation.

The oxidative degradation mainly occurs due to the presence of O_2 or metal ions in the flue gas. The absorber is prone to oxidative degradation due to its high level of CO_2 concentration(Chiet.al.,2002).

Thermal degradation occurs mainly at high temperature. CO_2 loading and amine concentrations strongly influence the rate of thermal degradation. High temperature breaks the chemical bonds of amines, increasing the reaction rate of amines with CO_2 to form thermal degradation products. Atmospheric degradation is a complex process and gives a wide range of products in comparison with oxidative and thermal degradation. This type of degradation is initiated by the reaction of amine with –OH radicals. The –OH radical abstracts the hydrogen from the CH and NH groups to generate amine radicals. After the initiation of radicals, they further react with present chemicals to form degradation products (Lepaumier et al., 2009).

1.3 Impacts of amine vapourization loss

The amines emitted into the atmosphere are highly unstable and undergo various side reactions to form degradation products. The aliphatic amines containing –OH radicals initiate atmospheric degradation and form products such as aldehydes, amides, nitrosamines, and nitramines. Different amines form different atmospheric degradation products. MEA on atmospheric degradation undergoes initial hydrogen abstraction to form formamide, 2-hydroxy-acetamide, and some peroxyacetyl-nitrates and other amides. The end products of AMP atmospheric degradation are N-nitro-formamide, acetamide, nitrosamines, and nitramines. MDEA degradation forms amides and polyacrylonitrile (PAN)-like compounds, whereas for piperazine, 2-piperazinone and amides in addition to nitrosamine and nitramine are formed. The amines and the degraded products have a major impact on the environment, health and economy of the amine plant. The impacts

depend on the type of amine used in the process and the amount of amine emitted into the atmosphere. Amine volatility, quantified by the parameter γ, between $0.45 < \gamma < 0.55$ was proven to be a concern in the CO_2 capture process in perspective of health, environment and economy (McLees, 2006).

1.3.1 Impact on the environment

Amines emitted into the atmosphere have an adverse effect on the environment. Biodegradability and eco-toxicity have to be considered during the assessment of environmental impact of amines in the environmental system. Amine biodegrades in soil and soil water into nitrogen components. Increased nitrogen decomposition leads to eutrophication, increasing biomass production, and reducing plant biodiversity. MEA has high biodegradability and has less impact on the environment in comparison to amines such as MDEA, AMP, and piperazine that have low degradability and long persistence in the environment. But the airborne emissions generated through MEA decomposition, such as nitrogen (N_2) and ammonia (NH_3), contribute to acidification and eutrophication in water bodies (Shao and shangeland, 2009).

Amines react with sulphuric acid ($H_2SO_{4)}$ and nitric acid (HNO_3) in the presence of sunlight to from aerosols and secondary particulates. They also form ozone in combination with nitrogen oxide compounds (NOx) and sunlight. Volatile organic compounds (VOCs) are one of the main constituents causing global warming. Carcinogenic products such as benzene are formed due to the emission of amine into the atmosphere (McLees, 2006). Nitrosamines are carcinogenic and also have an effect on

aquatic organisms. Table 1.1 gives the critical concentration responses of amines and degraded products on fish, algae and other invertebrates.

1.3.2 Impacts on health

An overall perusal of literature shows that over-exposure to amines and their degradation products have toxic effects on human health. The general effects are irritation, sensitization, carcinogenicity, and genotoxicity. The toxicity of amines varies considerably. The most commonly used MEA has an indication of reproductive and developmental toxicity. PIPA has a sensitizing and toxic effect on human health. It also causes blurred vision, coughing, and skin rashes after long exposure (McLees, 2006). Table 1.2 gives the exposure concentrations of different amines in air. The population should not be exposed overtime to levels higher than the reported concentrations.

Degraded products formed by the emission of amine into the atmosphere have a major impact on health. Formaldehyde is genotoxic and leads to cancer in the presence of a cytotoxic component. The threshold level for concentration of formaldehyde in the indoor environment set by the Norwegian Board of Health supervision is 100 μg/m^3. Formamide can cause cancer and affect reproductive ability. The threshold limit for formamide is set to be 24μg/L. Nitrosamines have carcinogenic effects on human health and injure the liver on exposure to N-nitrosodimethylamine (NDMA). Nitramines are mutagenic, and the long-term exposure limit is set as 4ng/m^3 (Shao and Stangeland, 2009). Only limited literature is available on the toxicity of amines on human health. It is important to assess more information to prevent long-term effects of amine emissions.

Table 1.1: Critical concentrations for amine and amine degradation products (Shao and Stangeland, 2009)

Group	Test	MEA (mg/L)	AMP (mg/L)	PIPA (mg/L)	MDEA (mg/L)	Amides (mg/L)	Nitrosamine (mg/L)	Nitramine (mg/L)
Fish	Acute	20	100	52	100	5000 Formamide	5.85	3.6
	Chronic	-	-	20	0.5	-	200	0.2
Invertebrate	Acute	83.6	100	230	10	13 Formamide	7.76	6.01
	Chronic	-	-	-	-	1.2 Formamide	100	0.4
Algae Bacteria	Acute	6	20	13	20	49 Acetamide	-	3.2
	Chronic	0.75	-	-	-	6600 Acetamide	0.025	-

Table 1.2: Exposure concentrations of amines in air (Shao and Stangeland, 2009)

Amine type	**Concentration** $(\mu g/m^3)$
MEA	10
AMP	6
MDEA	120
PIPA	5

1.3.3 Impacts on plant economy

Certain amounts of amine vapourization loss are unavoidable during operation. Significant losses of the solvent have a negative impact on the plant economy. The greater the amount of amine lost into the atmosphere, the greater the makeup cost of amine. This involves purchase of amine and directly attributes to an important economic issue. Amine loss greater than 40-50 ppm can be calculated as a very large economical loss by comparing the price of MEA purchased and CO_2 captured (McLees, 2006).In most amine operating units, a water wash is implemented to reduce the loss, but avoidance of the excessive amine loss results in a greater capital cost in the design of water wash (Nguyen et al., 2010).

1.4 Literature review on vapourization loss of amine

Stewart and Lanning in 1994 studied and predicted the vapourization loss for MEA, DEA, and MDEA. The results showed that MEA is much more volatile in comparison to MDEA and AMP. Table 1.3 illustrates the vapourization loss of amines per MMscf treatment of gas under absorber conditions of 700 psia and 120^{o}F. McLees in 2006 studied the equilibrium partial pressure of MEA, PZ and water using FTIR analysis at 35-70^{o}C. Few other studies include the work done by Closmann et al. in 2009. They studied volatility measurements on loaded MDEA/PZ using a semi-batch reactor apparatus and FTIR spectrometer. This study was conducted to measure the volatility of MDEA in various MDEA/PZ blends at 40^{o}C and 60^{o}C over the range of tested loading. The activity of PZ decreased with the increase in loading. The activity of PZ was high at 60^{o}C for MDEA/PZ blend under the loading conditions.

Table 1.3: Estimated vapourization losses in absorber and regenerator (Stewart and Lanning, 1994)

	Type of amine	**Estimated loss (lb/MMscf)**
ABSORBER	MEA (15%)	0.54
	DEA (30%)	0.004
	MDEA (30%)	0.035
	MDEA (50%)	0.061
REGENERATOR	MEA	<0.1
	DEA	<0.01
	MDEA	<0.001

The latest study on volatility was by Nguyen et.al in 2010. They studied only the volatility of 7m MEA, 8m PZ, 7m MDEA, 12m EDA, 5m AMP, 7m MDEA/2m PZ using Fourier Transform Infrared spectroscopy (FTIR) at 40-60^{o}C with lean and rich loadings and CO_2 partial pressures of 0.5 and 5kPa at 40^{o}C . They stated that the amine volatility can be represented by its apparent activity coefficient in a loaded system. As the CO_2 loading increased the volatility or the activity coefficient decreased as the free amine was consumed by CO_2. They concluded that 7mMDEA/2m PZ is the least volatile system with respect to the volatility at the nominal loading followed by 8m PZ, 12m EDA, 7m MEA and 5m AMP.

1.5 Research motivation and objective

From the literature review, it is evident that only Stewart and Lanning emphasised the study of amine loss due to vapourization using vapour pressure data. Other available literature measured the volatility of amines and obtained the vapour pressure data mainly for model predictions and vapour-liquid equilibrium. Thus, the research gap in measuring the amine vapourization loss highlights the need to focus on quantifying amine vapourization loss. Considering the effects of amine emission mentioned earlier, quantification of the loss and the factors involved in the loss becomes a major scope of study.

Therefore, this study aims at:

- Generating experimental vapour pressure data for mono-ethanolamine (MEA) using conditions that have previously been studied to a lesser extent;

- Substantiating a relation for activity coefficient of amine using a wide range of vapour pressure data as a function of amine concentration;
- Developing an easy-to-use empirical correlation for quantifying the amine vapourization loss as a function of plants operating condition; and
- Studying the behaviour of amine loss with respect to the process parameters.

LITERATURE REVIEW AND FUNDAMENTALS

2.1 Literature review on vapour pressure

As amine vapourization loss can be calculated from the solvent-based vapour pressure data, a thorough perusal of the literature was done to check the availability of vapour pressure data at various operating conditions of amine systems. Table 2.1 gives consolidated literature data of vapour pressure of pure, binary, and ternary amines at different conditions of temperature, pressure and concentration.

Nath and Bender (1983) measured the total pressure and the vapour pressure of binary solutions at temperatures between 60^{o}C and 95^{o}C. The binary solutions were monoethanolamine and water measured at 60, 78, and 92^{o}C, water-propanolamine at 75, 85, 95^{o}C, water-ethylene glycol at 65, 78, 90^{o}C, ethanol-ethanolamine at 65, 75, 80^{o}C, and propanol-propanolamine at 75, 85, and 95^{o}C. Only the total pressure of a liquid with known composition at constant temperature was obtained. The experimental vapour pressure data was obtained using a static device, and the liquid phase activity coefficient was determined using Wilson and UNIQUAC.

Xu et al. (1991) studied the vapour pressure of MDEA using a modified ebulliometer at temperatures between 55 and 108^{o}C and at concentrations ranging from 10 to 70 wt%. The vapour pressure of the solution was estimated using Raoult's Law.

Cai et al. (1996) studied the binary VLE of MEA + H_2O at pressures of 101.33 and 66.66 kPa and DEA+H_2O, MEA+DEA at a pressure of 6.66 kPa. The boiling temperature was measured using a modified Rose Williams still. The standard curve of refraction index and mole fraction of the binary mixture was used.

Table 2.1: Vapour pressure of amine systems

Reference	Amine system	Type of amine	Temperature (K)	Pressure (kPa)	Experimental Device
Nath and Bender (1983)	Binary	H_2O -Ethylene Glycol H_2O -MEA H_2O -propanolamine Ethanol-MEA Propanol-propanolamine	338, 351,363 333,351,365 348,358,368 338,348,358 348,358,368		Static device
Xu et al. (1991)	Binary	MDEA+ H_2O	330-369 329-374 326-374 334-377 332-381		Modified ebulliometer
Cai et al. (1996)	Binary	Ethanol+ H_2O H_2O +MEA H_2O +MEA H_2O +DEA MEA+DEA	 373-443 362-431 311-459 374-459	101.33 101.33 66.66 6.66 6.66	Modified Rose Williams
Park and Lee (1997)	Binary	MEA+ H_2O Ethanol+ MEA	373-443 351-443	101.3	Equilibrium apparatus
Tochigi et al. (1999)	Pure	MEA dimethylsulfoxide	358-440 356-462	3-90 2-97	Rogalski+ Malanowski
	Binary	H_2O +MEA MEA+ dimethylsulfoxide H_2O +dimethylsulfoxide	363 363 363	4-70 3-4 3-70	
	Ternary	H_2O + MEA + dimethylsulfoxide	363	5-56	
Abdi and Meisen (1999)	Binary	DEA+H_2O	309-405		Dynamic ebulliometer
Horstmann et al. (2002)	Pure	2,2'-diethanolamine Methanol H_2O	401-541	0.41-100	Dynamic ebulliometer
	Binary	Methanol+2,2' diethanolamine H_2O +2,2'diethanolamine	365 365	0.03-272 0.04-75	
	Ternary	Methanol+2,2'diethanolamine+ H_2O	313,333,353, 374,313,333,353,373		
Voutsas et al. (2004)	Pure	H_2O	349, 356, 362	40,53,67	Modified ebulliometer
	Binary	H_2O +MDEA	349-459	40,53,67	

Kapteina et al. (2005)	Pure	MEA 2-(methylamino)-ethanol 2-(ethylamino)-ethanol 2-(dimethylamino)-ethanol 2-(diethylamino)-ethanol)	280-306 275-293 283-306 278-292 278-295		Transpiration method
McLees (2006)	Pure	MEA	324-327		FTIR analysis
	Binary	MEA+ H_2O Piperazine(PZ)+ H_2O	316-338 309-336		
	Ternary	MEA+PZ+ H_2O	310-334		
Pappa et al. (2006)	Pure	AMP	373-437		Modified Swietoslawski ebulliometer
	Binary	AMP+ H_2O	362-424 367-430 373-437	67,80,101	
Barreau et al. (2007)	Pure	AMP	365-425	5-70	Ebulliometer
	Binary	MDEA+ H_2O Methanol+AMP MDEA+methanol AMP+ H_2O		10,30,50,70,90 30,50,70,90,101	
	Ternary	Methanol+ MDEA+ H_2O H_2O +AMP+ methanol Methanol+AMP+ H_2O		30,50,70,90,101 30,50,70,90,101 30,50,70,90,101	
Kim et al. (2008)	Pure	MEA MDEA MAPA	357-435 410 327-412		Modified Swietoslawski ebulliometer
	Binary	MEA+ H_2O MDEA+ H_2O MAPA+ H_2O	313,333,353,373		
	Ternary	MEA+MDEA+ H_2O MDEA+MAPA+ H_2O	313,333,353,373 333,353,373		
Belabbaci et al. (2009)	Pure	MEA Methylmorpholine H_2O	283-363 273-353 283-364		Static devices
	Binary	MEA + H_2O 4-methylmorpholine + H_2O	283-363 313-363		
Park et al. (2009)	Binary	H_2O +MEA Methanol+ethanol H_2O + MEA	355-430 339-349 355-421 367-430	50 70 101.33 50 70	Stage Muller Dynamic circulating cell

Park and Lee (1997) measured boiling points and the equilibrium compositions of liquid and vapour phase for MEA+ water and MEA+ ethanol at atmospheric pressure using an equilibrium cell. The vapour pressures of pure compounds were calculated using Antoine's Equation. The liquid phase activity coefficient for non-ideal behaviour was calculated using Wilson, Non-Random Two Liquid (NRTL) and Universal Quasi Chemical (UNIQUAC) equations. The fugacity coefficient of the vapour phase was calculated using the virial equation of state with the second virial coefficient.

Tochigi et al. (1999) measured experimental vapour liquid equilibrium (VLE) at 90^{o}C for the ternary system MEA+ water+ dimethyl sulfoxide and its three constituent binary mixtures using Rogalski-Malanoski equilibrium still. Using the Antoine's Equation, average deviations between the experimental and calculated vapour pressures were obtained. Rejecting the non-ideal behaviour of the gas, the activity coefficient was assessed using Raoult's Law.

Abdi and Meisen (1999) measured vapour pressures of DEA-H_2O using a dynamic cell. The vapour phase was assumed to have ideal behaviour, and the liquid phase was assumed to have non-ideal behaviour. Activity coefficient models were used to correlate the VLE data.

Horstmann et al. (2002) reported the isobaric vapour-liquid equilibrium for pure component 2, 2'-diethanolamine, for binary systems (methanol+2, 2'-diethanolamine) and (water+2,2'-diethanolamine) and for the ternary system (methanol+2,2'-diethanolamine+water). For the pure component, the vapour pressure was measured using a dynamic ebulliometer at a temperature range of 128-268^{o}C. The boiling temperature of the component was measured while keeping the pressure constant. Using the

experimental data and the calculated data the coefficients of Antoine's Equation were fitted for the component.

Voutsas et al. (2004) measured the isobaric vapour liquid equilibrium of aqueous MDEA solution, using a modified ebulliometer at 40, 53.3 and 66.7 kPa, temperature ranging from 76-186^{o}C and concentration of the liquid MDEA ranging from 0.06 to 0.93 in mole fraction. The vapour pressure was calculated using the Clausius Clapeyron Equation (2.1)

$$\ln(P^{s}) = 26.13691 - \frac{7588.516}{T} \tag{2.1}$$

where P^{s} is the saturated vapour pressure (Pa) and T is the temperature (K).The data obtained through this study were used for fitting UNIQUAC temperature dependent interaction parameters.

Kapteina et al. (2005) studied the vapour pressure and the enthalpies of vapourization of monoethanolamine (MEA), 2-(methylamino)-ethanol (MAE) and 2-(dimethylamino)-ethanol (DMAE), 2-ethylaminoethanol, and 2-diethylaminoethanol using transpiration method. The saturation vapour pressure (p_i^{sat}) at each temperature obtained was fitted using Equation (2.2)

$$R\ln(p_i^{sat}) = a + \frac{b}{T} + \Delta_1^{g}C_p \ln\left(\frac{T}{T_o}\right) \tag{2.2}$$

$\Delta_1^{g}C_p$ is the difference between the molar heat capacities of the gaseous liquid and vapour phase, a and b are the adjustable parameters and T_o is the arbitrarily chosen reference temperature. The vapour pressure of 2-amino-ethanol was measured between 6-51.4^{o}C.

McLees (2006) worked on amine volatility for model predictions. He studied the partial pressures of MEA and piperazine (PZ) at temperatures between 35 and 70^{o}C using the stirred reactor. The gas partial pressure for the binary system (MEA-H_2O) was

measured for pure MEA, 23.8m MEA, 7m MEA and 3.5m MEA at temperatures 35, 45, 55, and 65^{o}C .The results were compared with pure liquid vapour pressure in the form of Equation (2.3) given below:

$$p_i^{sat} = A + \frac{B}{T} + C \ln T + DT^E \quad (2.3)$$

p_i^{sat} is the vapour pressure (Pa) of the component i, T is the temperature (K), and A, B, C, D and E are the constants. The results obtained showed that 7m MEA solution had higher relative volatility than 3.5m MEA. The emissions of MEA and PZ from the absorber were 45 and 8 ppm, respectively.

Pappa et al. (2006) presented the vapour pressure data of pure 2-amino-2-methyl-1-propanol (AMP) and binary (AMP+H_2O) at a temperature range of 89-164(K) and at pressures of 66.7, 80 and 101.3(kPa), using a modified Swietoslawski ebulliometer. Vapour pressure was correlated with Antoine's Equation (2.4) as follows:

$$\ln(P^s) = 15.155 - \frac{3472.6}{T-107.32} \quad (2.4)$$

where T is temperature (K) and P^s is the vapour pressure (kPa). The activity coefficient was calculated from Raoult's Law, and the fugacity coefficient and Poynting term were taken as unity since low pressure was involved.

Barreau et al. (2007) measured vapour pressures of pure AMP and binary solution consisting of MDEA+H_2O and Methanol AMP using an ebulliometer for a wide range of temperatures, pressures and concentrations.

Kim et al. (2008) generated experimental data at 40, 60, 80, and 100^{o}C and compositions of two phases (P, T, x, y) for pure, binary and ternary solutions of monoethanolamine (MEA), N-methyldiethanolamine (MDEA) and 3-(methyl amino) propylamine (MAPA). The vapour pressure of pure MEA, H_2O, MDEA, and MAPA

were measured using the Modified Swietoslawski ebulliometer and fitted with the Antoine's Equation to calculate the activity coefficient using Equation (2.5):

$$\gamma = \frac{y_i P}{x_i p_i^{sat}} \varphi_i \tag{2.5}$$

x_i and y_i are the liquid and vapour phase mole fractions. p_i^{sat} is the vapour pressure of the pure component i, P is the total pressure, γ is the activity coefficient, and φ_i is the fugacity coefficient. At low to moderate pressure , φ_i is avoided as it is of least importance, and the activity coefficient was fitted to the Wilson and NRTL equations.

Belabbaci et al. (2009) measured the vapour pressure of monoethanolamine and water (MEA+H_2O), 4-methylmorpholine and water, and pure components using a static device at temperatures between 10 and 90^oC. The saturated vapour pressure p_i^{sat} (kPa) data were correlated with the Antoine's Equation (2.6) given as:

$$\log(p_i^{sat}) = A - \frac{B}{C+T} \tag{2.6}$$

T is temperature (K) and A, B, and C are constants. The experimental vapour pressures (p_i^{sat}) data for pure water and the binary solution were obtained as functions of temperature (T) and constant mole fraction (x_i).The data obtained were used to calculate excess Gibbs functions and were fitted to the fourth order Redlich Kister equation using Barker's method. The literature concluded that the deviations from Raoult's Law were negative for the binary solution of MEA and H_2O.

Park et al. (2009) measured the isobaric vapour-liquid equilibrium data using a modified Stage-Muller equilibrium still for MEA+H_2O. The data were obtained for pressures of 50 - 70 kPa and temperatures of 82.2 - 157.3^oC. The activity coefficient for liquid phase at low pressure was calculated using the following Raoult's Law Equation:

$$\gamma x_i p_i^{sat} = y_i P \tag{2.7}$$

where x_i and y_i are the liquid and vapour phase mole fractions, respectively. p_i^{sat} is the vapour pressure of the pure component I, P is the total pressure, and γ is the activity coefficient. The vapour pressures of pure components were obtained using the Korean Database Equation (2.8) given below.

$$\ln(p_i^{sat}) = A\ln(T) + \frac{B}{T} + C + DT^2 \quad (2.8)$$

The experimental data were correlated using the NRTL and UNIQUAC models.

Nguyen et al., (2010) studied the effect of CO_2 loading on the activity of amines. The effect of CO_2 loading on amine activity for MEA concentrations of 3, 7, and 11m and temperature 40 and 60^oC is shown in Figure 2.1. In a CO_2-loaded system, activity coefficient varied between 0.1 - 0.5 mol/mol. The volatility of amine in terms of activity coefficient decreases as the CO_2 loading increases. This is due to the fact that less active amine is present in the solution as most of it is involved in the consumption of CO_2. In Figure 2.2, under the same experimental conditions the activity coefficient as a function of whole MEA concentration in terms of mole fraction between 0.05 to 0.175 and CO_2 loading varying between 0.1 - 0.5 mol/mol, the behaviour of CO_2 loading does not seem to affect the activity coefficient.

2.2 Raoult's Law

Raoult's Law states that the vapour pressure of a solution is dependent on the vapour pressure of each chemical component and the mole fraction of the component present in the solution. Equation (2.9) is the total vapour pressure of the solution, when the solution reaches equilibrium,

$$P = (p_a^* \times x_a) + (p_b^* \times x_b) + \cdots (p_i^* \times x_n) \quad (2.9)$$

Figure 2.1: Behaviour of activity coefficient with CO_2-loaded MEA solution

Figure 2.2: Behaviour of activity coefficient (γ) with whole concentration MEA (x_i)

and Equation (2.10) gives the vapour pressure of the individual component,

$$p_i = p_i^* \times x_i \tag{2.10}$$

p_i is the partial pressure of the component i in the solution and $x_a, x_b, \text{and } x_i$ are the mole fractions of the component present in the solution. p_i^* is the vapour pressure of the pure component. This law is valid only for idealized kinds of solution. The behaviour of real gases can be explained in a close approximation of idealized kind of gases. The real solution departs from the ideal to greater or lesser degrees depending on the similarity of the component molecules. The basis for ideality is that the molecules in both components should be identical. The interaction between the like and the unlike molecules should be the same. An ideal mixture is one in which the chemical potential of each of its constituents is given as:

$$\mu_i = \mu_i^0 + RT \ln x_i \tag{2.11}$$

where μ_i is the partial molar Gibbs energy called chemical potential, and μ_i^0 is the chemical potential of the pure solvent *i* in the solution. The solutions whose components follow the above equation at all the composition ranges and temperatures are truly ideal solutions and have no change of volume or heat while mixing (Klotz and Rosenberg, 1994).

When the system reaches equilibrium, the chemical potential of the component present in liquid and vapour states must be the same, i.e.,

$$\mu_{i,liq} = \mu_{i,vap} \tag{2.12}$$

In order to make use of the above equation in measurable quantities (T, P), ideal gas law for the partial volume term is substituted in Gibbs Duhem Equation to arrive at:

$$\mu_i - \mu_i^0 = RT \ln \frac{P}{P^o} \tag{2.13}$$

Since the above equation is too limiting, pressure was replaced with fugacity.

$$\mu_i - \mu_i^0 = RT \ln \frac{f}{f_i^o} \tag{2.14}$$

The above equation allows measurement for multiple non-ideal phases. Further, the fugacity ratio was defined as activity shown below.

$$\frac{f_i}{f_i^o} = a_i \tag{2.15}$$

The above equation was applied in Equation 2.12 as a new term for equilibrium given as:

$$f_{i,liq=}f_{i,vap} \tag{2.16}$$

The fugacity can be replaced by pressure if the behaviour of the solution is ideal.

$$p_i = x_i\, p_i^* \tag{2.17}$$

The above expression (2.17) is known as Raoult's Law and is used in defining an ideal mixture (Smith, 1973).

2.2.1 Raoult's Law and ideal mixture of liquids

Consider two liquids, A and B, each making its own contribution to the overall vapour pressure of the mixture. If the mole fraction of A in the mixture is doubled, the partial pressure of A is doubled according to Raoult's Law. The partial pressure of the component is proportional to the mole fraction. If the partial pressure is plotted against the mole fraction we get a straight line. Conversely, the mole fraction of B falls steadily with the increase in mole fraction A. The vapour pressure of B decreases as well. If the vapour pressure of B is higher than that of A, it means that the molecules tend to break away more easily from B than A and B happens is then more volatile than A and vice-versa. The total pressure is obtained by the addition of both A and B for each composition. If a liquid has higher vapour pressure, it means that the liquid molecules

have higher tendency to escape more into the vapour phase, and, therefore, it does not require a high supply of heat. Thus, high vapour pressure molecules have low boiling points. If the vapour pressure of a liquid is low, it means that the boiling point will be high as it requires a high amount of heat to break the molecular bonds (Smith, 1973).

2.2.2 Dilute solutions

In dilute solutions, solvent usually follows Raoult's Law and solute does not. As the solution gets diluted, the solvent molecules are surrounded by the same molecules whereas the solute is surrounded by more solvent molecules, which is, thus, not related to a pure liquid solute and hence does not follow Raoult's Law. The partial vapour pressure might be a linear function of mole fraction in dilute solution, but the constant of proportionality is not the vapour pressure of the pure solute p^* but, rather, is just an arbitrary constant. If a solute has a partial pressure proportional to its mole fraction, it is said to follow Henry's Law. Hence, Henry's Law states that the vapour pressure of the solute is proportional to the solute's mole fraction, but the constant of proportionality is different and must be determined experimentally(Stadler, 1989).

2.2.3 Non-ideal case behaviour

For many real solutions, Raoult's Law and Henry's Law do not hold for the solvent and solute, respectively. In such cases, the concept of activity is introduced. Unlike gases, liquids rarely form ideal mixtures due to the proximity of their molecules. Non-ideal behaviour is generalised as:

$$\mu_b = \mu_b^- + RT \ln a_i \qquad (2.18)$$

a_i is the activity of the substance in the mixture

$$a_{i=}x_i\gamma_i \tag{2.19}$$

γ_i is the activity coefficient

The effective concentration in real solutions differs greatly from the true concentration due to the interaction between molecules. The extent to which this is measured is by the activity coefficient γ_i. The correction factor, called the activity coefficient, is used for relating ideal and non-ideal behaviour.

$$\gamma_i = \frac{a_i}{x_i} = \frac{\text{Effective concentration}}{\text{Real concentration}} = \frac{f}{xf^*} \tag{2.20}$$

In an ideal solution, taking the pure state as the reference state x_i=1, a_i= 1, $\gamma_i = 1$.

When the effective concentration is less than the real concentration, the activity coefficient is less than 1. This shows the lower tendencies of molecules to escape into the vapour phase, and, hence, the components would deviate negatively from Raoult's Law. If the components deviated positively from Raoult's Law and had vapour pressures greater than the law would predict, then $a_i > x_i$ and $\gamma_i > 1$. This indicates repulsion leading to the separation of two immiscible layers. Most normal liquid mixtures in which the components do not interact well with each other tend to escape into the vapour phase (Reid, 1990).

The liquid phase non idealities is defined in terms of activity coefficient.

$$\gamma = \frac{a_i}{x_i} = \frac{f_i^L}{x_i f_i^o} \tag{2.21}$$

$$f_i^L = \gamma x_i f_i^o \tag{2.22}$$

where activity coefficient is the ratio of activity and concentration of component i in the solution, and f_i^o is the standard state fugacity of pure liquid component i in the solution.

Fugacity coefficient is defined as the pure component vapour pressure p_i^o for the compounds which are liquids at standard conditions at the temperature of the system.

$$f_i^L = \gamma x_i P_i^o \int_{p_i^o}^{P} \frac{v_i dP}{RT} \quad (2.23)$$

The integral term added refers to the Poynting correction term for system pressures that are different from the saturation pressure. The Poynting correction term is close to 1 and is neglected in relatively low pressure in acid gas vapour liquid equilibrium. In case of no chemical reaction occurring in a system, the above reaction reduces to Raoult's law. In case of a non-ideal system, a method is devised for calculating activity coefficient in terms of composition and temperature. One way is to develop an empirical equation and fit the experimental data or to create a model for Gibbs energy relating to activity coefficient The fugacity coefficient is used for the vapour phase non-ideality and it is defined as the ratio of the fugacity coefficient in the vapour phase with its ideal gas partial pressure given below.

$$f_i^v = \varphi_i y_i P \quad (2.24)$$

Empirical equation of state is used in order to relate fugacity coefficient with measurable quantities (Posey, 1996).

2.3 Measurement of equilibrium data

Equilibrium data such as temperature, vapour pressure, composition of liquid and vapour phases can be determined using different methods and apparatuses. These methods are classified under two different categories, high and low pressure. However, choosing the appropriate method is a difficult task (Rogalski and Malanowski, 1980). Static, circulation and dynamic are the methods discussed in this study. Static method is

simple and is considered to give highly accurate measurements (Rogalski and Malanowski, 1980), but the main drawbacks of this method are the necessity of degassing of samples, the expensive equipment, and the long term duration before reaching equilibrium (Rogalski and Malanowski, 1980). Vapour pressure measurement is done after complete degassing of the equipment or else it is subject to large errors. At very low pressures, there is a pressure drop in the equipment. Therefore, the static method is not suitable for low and moderate pressures, but for high pressures, this method is considered to give accurate results (Kim et al., 2008).

Temperature, pressure, and composition of vapour and liquid phases can also be determined using circulation method. The basic principle behind this method is the separation of liquid and vapour phases under steady state conditions and the vapour phase re-circulating back to the liquid phase (Malanowski, 1982). The circulation method is widely used in the range of medium and low pressures, but the difficulties in attaining steady state and problems arising in system with limited miscibility in the liquid phase led to the development of dynamic flow method (Kim et al., 2008).

Dynamic method is carried out under isobaric conditions where the pressure is kept constant and the boiling point is determined, whereas in static method, the pressure is determined at constant temperatures. The dynamic method uses an ebulliometer for precise measurement of boiling point of liquids (Kim et al., 2008). For this purpose, an ebulliometer with a thermal lift pump to carry the boiling liquid to a thermometer was initially introduced by Cottrell, which was further modified by Swietoslawski and Romer . Gillespie (1946) introduced further modifications to the Swietoslawski ebulliometer by the addition of a separator for separation of liquid and condensate and for the withdrawal

of liquid and condensate phase without interrupting the boiling. Different authors introduced different modifications to the apparatus in order to avoid major drawbacks. Various studies led to the confirmation that reliable vapour pressure data and boiling temperature measurements have been obtained using the Swietoslawski ebulliometer (Rogalski and Malanowski, 1980). The modified Swietoslawski ebulliometer is considered more accurate for the determination of boiling point at pressures ranging from 5 - 200 kPa.

2.4 Swietoslawski ebulliometer

The accurate data produced using the Swietoslawski ebulliometer enable the apparatus to be used for measuring vapour pressure data. It is also designed for the measurement of boiling point, total pressure, composition of liquid, and vapour phases, so temperature and pressure of amine system can be determined with one (Rogalski and Malanowski, 1980). The main purposes of an ebulliometer are infinite dilution activity coefficient measurement, high pressure measurements, measurement of solubility limits and screening of azeotropic systems (Olson, 1989).

There are two different methods to determine the equilibrium parameters using an ebulliometer, i.e. complete and total pressure methods. The complete method deals with the determination of vapour and liquid phases simultaneously. The liquid and vapour samples are withdrawn from the apparatus without affecting the boiling. They are withdrawn through the septums' containing the liquid and vapour phases using a syringe. Usually, the liquid sample is withdrawn before the vapour phase. The accuracy of the results depends on the sample withdrawal and analysis. In the total pressure method, the

liquid sample is of known composition and the temperature and pressure are determined. Once the method of determination is chosen, the experiment can be carried out either under isobaric or isothermal conditions. Under isobaric conditions steady state is reached within a few minutes of change in sample composition. Under isothermal conditions pressure in the system is adjusted until the proper temperature is reached. The method depends on the nature of the system investigated (Rogalski and Malanowski, 1980).

2.5 General behaviour of amine vapourization loss

It is commonly known that a CO_2 absorption column can be operated under ranges of operating and design conditions so as to achieve a specific CO_2 capture target. The important conditions include type of amine used in the absorption liquid and amine concentration, CO_2 loadings of lean amine entering the column and rich amine leaving the column, feed temperature of lean amine, composition (or CO_2 content), as well as the temperature of feed gas, and also CO_2 capture efficiency presented in terms of CO_2 removal percentage. All these conditions are clearly identified in a simplified diagram shown in Figure 2.3.

Figure 2.3: Important operating and design parameters for CO_2 absorption column

3. EXPERIMENTS

The experiments in this study were done using the Swietoslawski ebulliometer for measuring the boiling point of solutions. The infinite dilution activity coefficients were calculated using the boiling point measurements at isobaric conditions. Precise measurements and accurate results were obtained using this apparatus.

3.1 Experimental apparatus

Figures 3.1 and 3.2 show, respectively, a photograph and a schematic diagram of the Swietoslawski ebulliometer used in this study. The setup consists of a number of components including a vacuum pump, a water bath, a condenser, a pump, an equilibrium cell with a thermocouple, glass vessels, a long glass tube, an electrical heater, and pressure gauges.

- A self-cleansing dry vacuum pump model 2025 (9 Torr, 12 mbar), Welch, Gardner Denver product, USA, was used in this study. It can be operated between 12-60 kPa.
- A pressure gauge, AshCroft, CE0518, 60psi was used for pressure measurements.
- A polystat R6L digital refrigerated circulator was operated at a temperature range of 20 - 150^{o}C. It was designed to provide temperature control for applications requiring a fluid work area or pumping to an external system. The temperature stability is $\pm$0.05^{o}C.
- A shell and tube condenser was used during the experiment in order to recover the amine vapour back into the system. The condenser was double walled with inlet and outlet tube. The inner tube was spirally coiled for better condensation.

Figure 3.1 Experimental setup of the Swietoslawski Ebulliometer

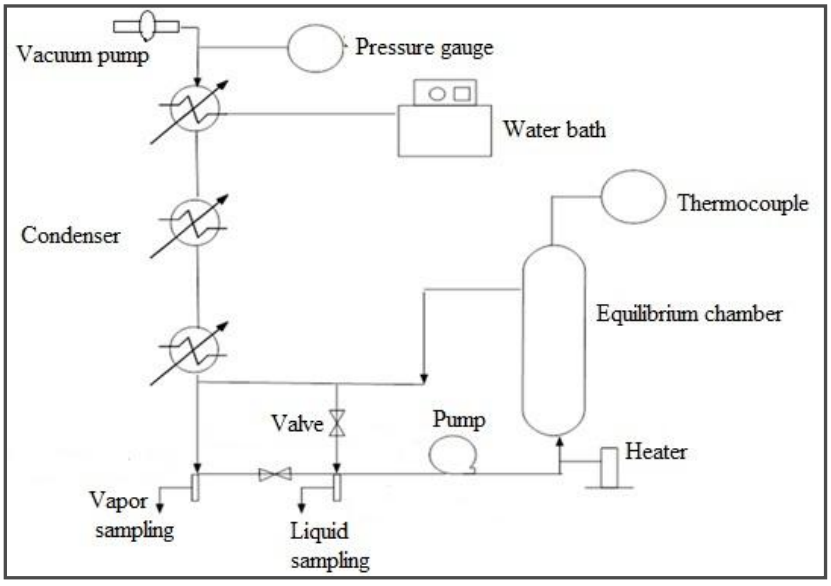

Figure 3.2 Schematic of the experimental set up used in this study

The length of the condenser was 45cm.

- A micro pump and a gear pump driver (Cole Parmer, WA, USA, model 75211-22) were operated at 40-3600 rpm to circulate the liquid and vapour samples into the system. The flow rate of the liquid was maintained by adjusting the speed of the pump.
- An equilibrium cell was made completely of glass to withstand high temperatures. A dual J-T-E-K thermocouple with an accuracy of $\pm$ 1^{o}C (Barnant, USA) was attached to the equilibrium cell to read the equilibrium temperature.
- Two glass vessels, 24/40 Chem glass, USA for the collection of condensed vapour and liquid were used in this system. The two glass vessels had three openings and one of the openings, was connected with a thermocouple to measure the temperature of liquid and condensed vapour phases.
- A packed column was used for the liquid to be pumped up to the equilibrium cell. The column was made of thick glass to withstand high heat, as it was connected to the heater to heat up the liquid flowing through the column. The column was packed with beads to enhance proper heat transfer during the flow of liquid.
- A heating mantle minder II (Glass-Col, Terre Haute, USA catalogue no 104A PL512) with a maximum load of 120 VAC, 15A, and 60Hz was used to heat up the liquid sample. The heating was facilitated with the help an adjustment knob.

3.2 Chemicals

Monoethanolamine (MEA) of 99% purity purchased from EM Science (Germany), was used for the sample preparation and validation of the system. Methyl orange of pH 3-4.4 was used as the colour indicator. 1N Hydrochloric acid (BDH) at 25^{o}C was used for sample titration.

3.3 Sample preparation

The amine solution was prepared by calculating the amount of amine with the desired concentration and the required volume of solution. Knowing the amount of amine and the density of amine, the mass of amine and volume of amine were calculated to get the desired concentration. The calculated volume of amine was taken and made up to the required volume using distilled water. The concentration was verified by titrating the solution with 1 kmol/m^3 standard hydrochloric acid and using methyl orange as the indicator.

3.4 Experimental procedure

150 ml of the known concentration of the solution was fed into the system. The liquid solution was allowed to pump up the long glass tube with the help of the pump and was maintained at a constant flow rate. The liquid was allowed to flow into the equilibrium cell and back to the container. A continuous flow of liquid solution was maintained in the system using a pump. The experiment was operated under iso-static conditions. The temperature of the solution was maintained by adjusting the pressure until the boiling point of the solution was reached. The pressure of the system was

observed using a pressure gauge connecting the system and the vacuum pump. The water bath was maintained at a very low temperature. The inlet and the outlet of the water bath were attached to the condenser, and a continuous flow of liquid was maintained. The system pressure was adjusted and the liquid was heated up with the help of the electrical heater. The heat supplied to the system was adjusted accordingly. The liquid attained its boiling state within 20 - 30 minutes. During the state of boiling, the liquid and the vapour were pumped to the equilibrium cell. The thermocouple attached to the equilibrium cell read the temperature corresponding to the boiling point temperature of the liquid. The liquid was collected by the holdup after it was passed through the equilibrium chamber, and the vapour was condensed along the walls of the condenser. After a particular interval of time, condensed vapour was collected at the condensed vapour hold up tube. The equilibrium state was observed when there was no change in temperature for a minimum of 10 minutes. Once the equilibrium temperature was attained, the heating was turned off and the system was cooled to allow the vapour to condense completely.

5 ml of the liquid and the vapour samples were taken using a syringe through the septum of the containers. The samples were titrated with the 1kmol/m^3 of standard hydrochloric acid using methyl orange as the indicator. The titration was carried out until concordant values were obtained. Using the titrated values, the concentrations of amine in the liquid and vapour phases were analyzed.

3.4.1 Analysis of activity coefficient

Knowing the concentrations of liquid and vapour phases, the mole fractions of MEA in the liquid and vapour phases can be calculated. Knowing the mole fraction and

the saturated vapour pressure (p_i^{sat}), the activity coefficient (γ) can be calculated using Raoult's Law. The p_i^{sat} data were calculated using Antoine's Equation given below:

$$\log(p_i^{sat}) = A - \frac{B}{C+T} \tag{3.1}$$

p_i^{sat} is the saturated vapour pressure of pure solvent (kPa) and T is the temperature (K). The p_i^{sat} calculated using the above equation was used to calculate the activity coefficient. Raoult's Law is given as:

$$x_i p_i^{sat} = y_i P \tag{3.2}$$

where x_i is the mole fraction of MEA in the liquid phase, y_i is the mole fraction of MEA in the vapour phase, and P is the total pressure (kPa). Using the above equation, the activity coefficient was calculated using the measured variables as follows:

$$\gamma = \frac{y_i P}{x_i \; p_i^{sat}} \varphi \tag{3.3}$$

As this study involved low to moderate pressure, the fugacity coefficient (φ) was neglected.

3.4.2 Validation of experimental technique and instrumentation

The experimental techniques and the instruments used in this work were validated to ensure the reliability of the data obtained. The validation was carried out by measuring boiling points of water under an isobaric condition and comparing the obtained boiling point values with the values from the literature. The validation results in Table 3.1 and Figure 3.3 show that the obtained boiling points are reproducible and in good agreement with the boiling points from the literature.

Table 3.1: Summary of boiling points of water

Kim et al. (2008)		**This work (run 1)**		**This work (run 2)**		**This work (run 3)**	
T(^{o}C)	**P(kPa)**	**T(^{o}C)**	**P(kPa)**	**T(^{o}C)**	**P(kPa)**	**T(^{o}C)**	**P(kPa)**
38	7	50	13	57	17	59	18
40	7	58	17	58	18	58	18
50	12	58	18	62	20	62	20
52	14	62	20	64	25	64	25
52	14	64	25	65	30		
60	20	65	30				
60	20	25					
60	20	30					

Figure 3.3 Boiling point of water

4. RESULTS AND DISCUSSIONS

4.1 Experimental results

This chapter begins with a discussion of the results from the experimental work done during this study. Table 4.1 gives the experimental vapour pressure data obtained for a binary solution of monoethanolamine (MEA+ H_2O). The experiments were carried out for a concentration range of 1-7 kmol/m^3. The conditions were chosen relevant to the industrial operating conditions. Low concentration range was prioritised as the availability of vapour pressure data in a low range of concentration in the literature was few. Analysis of liquid phase X_{mea} and vapour phase Y_{mea} amine was done at a constant temperature of 80^{o}C, and the vapour pressure of the solution was recorded at equilibrium. The liquid and vapour phase concentration of amine is represented in mole fraction. Using these data, the amine volatility was quantified using the activity coefficient (γ) obtained from a modified Raoult's Law:

$$\gamma x_i p_i^{sat} = y_i P \tag{4.1}$$

x_i and y_i are the MEA concentration in the liquid and vapour phase, respectively. P is the total vapour pressure of the solution. p_i^{sat}(kPa) is calculated using Antoine's Equation (4.2) and T(K) is the temperature.

$$\log(p_i^{sat}) = A - \frac{B}{C+T} \tag{4.2}$$

Using the A, B and C constants from literature operated at the same experimental conditions the coefficients for Antoine's Equation were fitted for the MEA component. The activity coefficient obtained for this study varied between 0.1-0.7. The negative deviation from Raoult's law shows that less amine was vapourized from the system.

Table 4.1: Experimental data for (MEA +H_20) binary system

T(^{o}C)	P(kPa)	x_{MEA}	y_{MEA}	γ_{MEA}
79.8	50.14	0.097	0.002	0.399
78.6	50.14	0.100	0.003	0.781
79.9	59.6	0.107	0.002	0.429
79.9	59.87	0.097	0.003	0.775
80.2	50.81	0.122	0.003	0.569
79.4	50.81	0.108	0.001	0.260
79.7	51.25	0.111	0.002	0.384
79.5	51.15	0.123	0.001	0.262
79.9	53.85	0.094	0.001	0.355
80.2	53.85	0.110	0.001	0.186
80.6	53.85	0.102	0.002	0.352
80.6	50.47	0.157	0.003	0.357
80.2	50.14	0.146	0.002	0.301
80.3	49.8	0.158	0.002	0.238
79.9	54.19	0.077	0.001	0.269
80.1	54.12	0.084	0.001	0.281
80.3	58.58	0.048	0.001	0.370
80.1	58.24	0.036	0.001	0.748
79.7	58.24	0.020	0.001	0.679
79.8	58.24	0.019	0.000	0.478
79.9	51.49	0.111	0.001	0.285
79.9	51.49	0.118	0.002	0.303
80.2	51.49	0.115	0.001	0.271
80.4	55.54	0.076	0.001	0.330
80.3	55.54	0.074	0.002	0.657
80.2	55.54	0.080	0.002	0.525
80.2	55.88	0.080	0.002	0.526
79.9	49.8	0.148	0.002	0.248
79.8	49.46	0.157	0.002	0.219
79.9	49.46	0.153	0.001	0.174
80.9	49.46	0.148	0.002	0.248

Experimental conditions such as temperature and pressure have an effect on the activity of amine. If the vapour pressure of the solution is high, the liquid starts boiling at a lower temperature and requires less supply of heat. If the vapour pressure is low, it requires more heat, and the solution boils at a higher temperature. Since the boiling point of MEA is high, the experimental conditions are maintained such that the solution boils at 80^{o}C, which means high vapour pressure is created in the system. In comparison of MEA to water, water boils at a much lower temperature. When the vapour pressure is increased, more water tends to escape than MEA, giving a very low activity coefficient for the low concentration range of MEA.

Figure 4.1 presents a graph in order to observe the behaviour off the activity coefficient as a function of concentration from the experimental data. It shows a highly scattered range of data indicating that the low concentration range chosen is very sensitive. These experiments require high order precision analysis to study the consistency of data. The measurement of data also depends on the equilibrium conditions. The activity coefficient obtained in this study was compared with those literatures in the low concentration range. The comparison is shown in Figure 4.2.The concentration range of MEA from other literature varied between 0.01 to 0.1 mole fractions. It is quite evident that at the low concentration range the activity of amine is not predictable. A survey of the literature shows that the study on activity coefficient at a low range of concentration is scarce and therefore more work is required to substantiate the behaviour of activity coefficient of MEA. Fig 4.3 shows the relation between the activity coefficient and the MEA concentration from a wide range of data from the literature gathered under

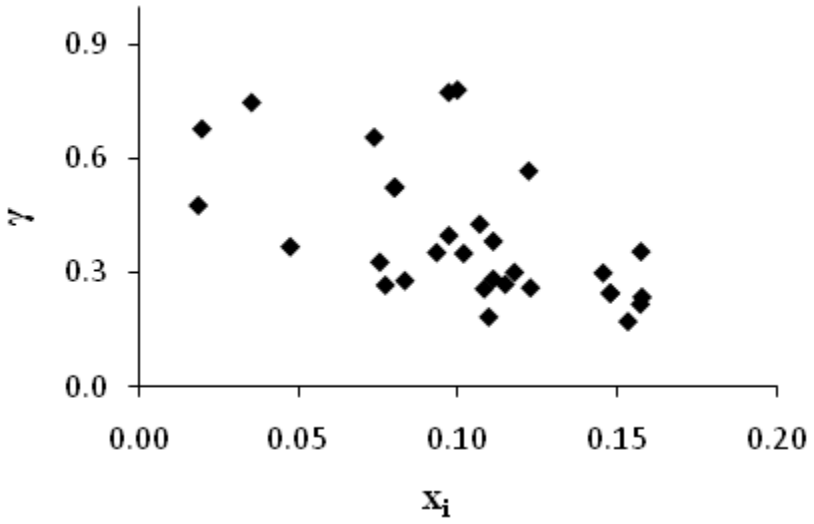

Figure 4.1: Activity coefficients of MEA (γ) from experimental work

Figure 4.2: Activity coefficient (γ) of MEA at a low concentration range (x_i)

Figure 4.3: Behaviour of activity coefficient (γ) with MEA concentration (x_i) from various data in the literature.

different conditions of temperature, pressure, and composition of MEA in the liquid phase..There is a clear trend in the activity of the amine with the concentration of MEA in the liquid phase. As there is no CO_2 in the system, there is free amine present in the solution. When the concentration of amine is increased, more amine tends to escape into the vapour phase as it is not involved in consumption of CO_2. Using the above information, an equation was regressed for the correlation between the activity coefficient and concentration of MEA in a system without CO_2 loading. Equation 4.3 correlates activity coefficient as a function of concentration of amine in the liquid phase obtained from Figure (4.4).

$$\gamma = (-0.4047(x_i)^2 + (1.1598\, x_i) + 0.3118) \tag{4.3}$$

γ is the activity coefficient of amine, and x_i is the concentration of MEA in the liquid phase. The derived equation was used in Raoult's Law to quantify the amine loss due to vapourization. Quantification of amine vapourization loss was calculated using the vapour pressure of MEA in the solution and the partial pressure of amine in the gas phase at certain temperatures and atmospheric pressure. The partial pressure of amine was obtained using Raoult's Law. Figure (4.5) shows regressed p_i^{sat} as a function of temperature using Antoine's Equation from the literature using same experimental conditions.. The significance of the activity coefficient is to modify the Raoult's Law so that it is applicable for both ideal and non-ideal cases. Equation (4.4) gives the correlation obtained for p_{isat} , the activity coefficient of the system as a function of temperature, MEA concentration, and pressure.

$$y_i = \frac{(-0.4047(x_i)^2 + (1.1598x_i) + 0.3118) \times (x_i) \times (3 \times 10^{-52} T^{20.39})}{P} \tag{4.4}$$

Figure 4.4: Regressed equation for correlation of mole fraction of MEA in the liquid phase and activity coefficient

Figure 4.5: Regressed equation for saturated vapour pressure (p_i^{sat})

P is total pressure; and yi and x_i are the mole fraction of MEA in the vapour phase and liquid phase, respectively. Thus, amine loss is calculated using the partial pressure of gas phase obtained from the empirical equation and gas flow rate (G).

$$\text{Amine loss} = (y_i P) \times G \tag{4.5}$$

where G is kmol/day. Equation 4.5 is used for the estimation of vaporization loss, and the effect of different parameters on the loss is discussed further.

4.2 Simulation of absorption column and its basis

In this study, amine loss from the amine scrubbing section was evaluated with the help of an in-house process model developed for gas absorption column. The process model was built according to the knowledge of heat transfer and mass transfer for the CO_2-amine system as well as the information on heat of reaction as to provide an insight into the changes in temperature of both gas and liquid streams as they travel through the column. From amine loss evaluation standpoint, temperature of gas stream leaving the column is considered the most crucial simulation result because it directly dictates vapour pressure of amine in the treated gas to be emitted to the atmosphere. The exit gas temperature is also important for determining an exact amount of water vapour leaving the scrubbing section. This piece of information is the key element for controlling water balance across the column.

In the present study, simulation of CO_2 absorption column was primarily based on capturing CO_2 from flue gas generated from the combustion of North Dakota lignite with 33% moisture. Excess oxygen of 5% for combustion was assumed in this study, thus

producing a hot flue gas that contains 13% CO_2 and 10% water vapour. Regardless of its source (either coal-fired or gas turbine stations), the hot flue gas was cooled prior to entering the absorption column to a specific temperature ranging from 15^{o}C to 40^{o}C. This cooling effect results in partial condensation of water vapour in the gas stream, leading to an increase in CO_2 concentration up to 14%. The absorption column in this work is set to remove CO_2 at a rate of 4 ton/day regardless of the removal efficiency of the column. The amine used in the scrubbing process was an aqueous solution of MEA with its concentration ranging from 3-7 kmol/m^3. Lean CO_2 loading was set to vary from 0.20 to 0.35 mol/mol while rich loading of up to 0.50 mol/mol was used during simulation. Feed temperature of MEA solution was 15-60^{o}C. In this study, the MEA concentration was set to be the same as the total MEA concentration accounting for both reactive MEA and MEA carbamate generated from CO_2 absorption reactions.

4.3 Parametric effects on amine vapourization loss

In this study, the amine used in the capture process was an aqueous solution of MEA with concentration ranging from 3.0 to 7.0 kmol/m^3 (or 18 to 43 wt %). The variation in amine vapourization with column operation was investigated through the changes in the following conditions.CO_2 loading of lean amine was varied between 0.15 and 0.35 mol/mol to cover the practical range while the loading of rich amine was varied between 0.40 and 0.45 mol/mol, which is close to the thermodynamic limit of a CO_2-MEA system. The feed temperature of lean amine was considered as the dependent variable controlled by the temperature of feed gas entering the bottom of the absorption column. The interconnection between liquid and gas temperatures exists especially when

the column operation is controlled in the water-balance mode where the amount of water vapour entering the column through feed gas must be equivalent to the amount of water vapour leaving the column with the treated gas. Keeping water balance is commonly done to maintain a constant concentration of MEA solution circulating within the process.

This practice makes feed gas temperature the important independent variable of the capture process. In this study, temperature of the feed gas was set between 20 to 60^{o}C in order to cover the typical value of 40^{o}C. The CO_2 content in the feed gas was based on two scenarios, i.e. coal combustion (approx. 13% CO_2) and natural gas combustion (approx. 8% CO_2). Excess oxygen of 5% for the combustion process was assumed in this study. It should be noted that the hot flue gas (after combustion) was cooled by scrubbing to the feed temperature prior to entering the absorption column, resulting in changes in moisture content of the gas stream. The variation in moisture content of the feed gas led to a variation in CO_2 content as shown in Table 4.2. The CO_2 capture efficiency was set at four values (i.e. 30%, 50%, 70% and 90%) so as to cover different levels of capture activity. The absorption column was set to remove CO_2 at a rate of 4.0 tons/day, regardless of capture efficiency. The following subsections report the effects of operating and design conditions on the amount of MEA that escaped through the column top.

4.3.1 Effect of rich and lean CO_2 loadings

Figure 4.6 shows how lean and rich CO_2 loadings of MEA solution have impacts on the amount of MEA vapour that could escape from the top of the CO_2 absorber. For

Table 4.2: Composition of feed gas at different feed conditions

Composition	**CH_4 Combustion**				**Coal Combustion (North Dakota's Lignite)**			
	Hot flue gas	**20°C**	**40°C**	**60°C**	**Hot flue gas**	**20°C**	**40°C**	**60°C**
CO_2 content (%)	7.24	8.31	7.83	6.78	12.88	14.04	13.24	11.54
O_2 content (%)	5.00	5.73	5.41	4.71	5.00	5.45	5.14	4.48
H_2O content (%)	14.48	1.90	7.84	19.36	10.01	1.90	7.48	19.36
Inert gas (%)	73.28	84.06	79.28	69.10	72.12	78.62	74.14	64.62

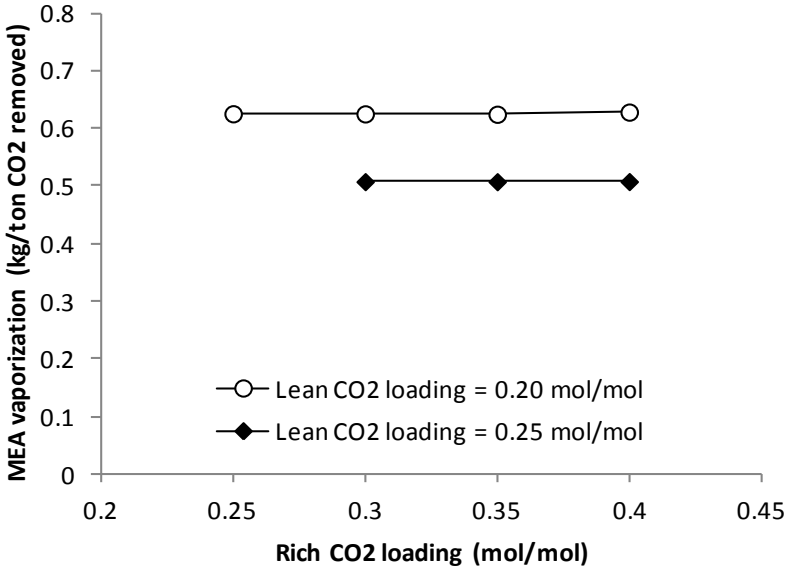

Figure 4.6: Effect of rich CO_2 loading (5.0 kmol/m^3 MEA solution; 90% capture efficiency; 40^oC feed gas; coal combustion)

given values of process conditions (including lean CO_2 loading, MEA concentration, feed temperatures of liquid and gas streams, gas composition and flow rate, and CO_2 capture efficiency), changing the rich loading results in only a variation in flow rate of MEA solution entering the absorber top. It, however, makes no impact on the properties of lean solution, especially MEA's vapour pressure. Thus it causes no changes in the level of amine vapourization. Unlike rich CO_2 loading, lean CO_2 loading has a great impact on the vapourization of MEA. As can be seen more clearly in Figure 4.7, raising CO_2 loading of lean MEA solution from 0.15 mol/mol to 0.35 mol/mol causes the amine vapourization to drop by more than 60% regardless of feed gas temperature and flue gas type (coal-based or CH_4-based). The reduction in vapourization level is a result of the reduction in concentration of active MEA available in the absorption liquid. By considering the carbamate formation (Eq. 4.6), which is the most dominant reaction for CO_2 absorption below 0.50 mol/mol loading (Astarita et al., 1983), each mole of absorbed CO_2 consumes two moles of reactive MEA ($OH\text{-}CH_2\text{-}CH_2\text{-}NH_2$) to form protonated MEA ($CH_2\text{-}CH_2\text{-}NH_3^+$) and MEA carbamate ($CH_2\text{-}CH_2\text{-}NH\text{-}COO^-$). An increase in CO_2 loading of amine solution causes the amount of reactive MEA in the liquid phase to decrease in a linear manner, leading to a linear reduction of MEA vapour pressure in the gas phase according to Raoult's' Law .

$$CO_2 + 2\ OH\text{-}CH_2\text{-}CH_2\text{-}NH_2 \leftrightarrow CH_2\text{-}CH_2\text{-}NH_3^+ + CH_2\text{-}CH_2\text{-}NH\text{-}COO^- \quad (4.6)$$

4.3.2 Effect of MEA concentration

As mentioned in the previous subsection, the amount of reactive amine in MEA solution has an impact on the level of MEA vapourization at the absorber top. The

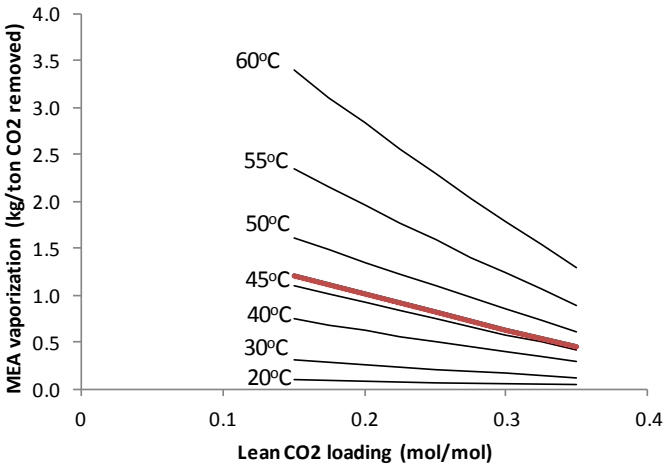

(a) Coal combustion

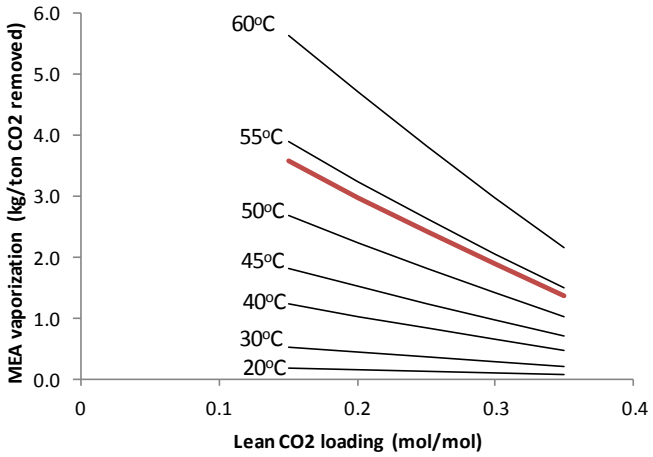

(b) CH_4 combustion

Figure 4.7: Effect of lean CO_2 loading at different feed gas temperatures (5.0 kmol/m^3 MEA solution; 90% capture efficiency; 0.40 mol/mol rich CO_2 loading)

concentration effect is also demonstrated in Figure 4.8 for MEA concentrations ranging from 3.0 to 7.0 kmol/m^3. This range of concentration was selected so as to cover the conventional operating conditions (5.0 kmol/m^3) as well as highly-concentrated solution (7.0 kmol/m^3). It appears from the figure that an increase in MEA concentration results in a higher amount of MEA vapour escaping through the column due to the higher MEA vapour pressure in the exit gas. It also can be noticed that the amine vapourization increase in direct proportion with MEA concentration. In other words, the effect of concentration is more pronounced as the MEA concentration continues increasing. For instance, a lean loading of 0.15 mol/mol, raising MEA concentration from 5.0 to 7.0 kmol/m^3 leads to an increase in vapourization of 0.59 kg/ton CO_2 whereas an increase in concentration from 3.0 to 5.0 kmol/m^3 results in an increase in vapourization of only 0.39 kg/ton CO_2.

The progressing effect of amine concentration is related to the change in temperature of the gas stream and amine solution passing through the absorption column. It is commonly known that CO_2 absorption into amine solution is an exothermic reaction where the heat of absorption is released to the liquid solution and a portion of the released energy is transferred to the gas stream inside the column. This common phenomenon demonstrates a form of temperature bulk along the absorption column as shown in Figure 4.9. It appears that, at the higher amine concentration, the temperature bulk is more pronounced and the average temperature of the column seems to be higher. The increasing column temperature with concentration is considered the primary cause of the progressive increase in MEA vapourization (and vapour pressure) in this case.

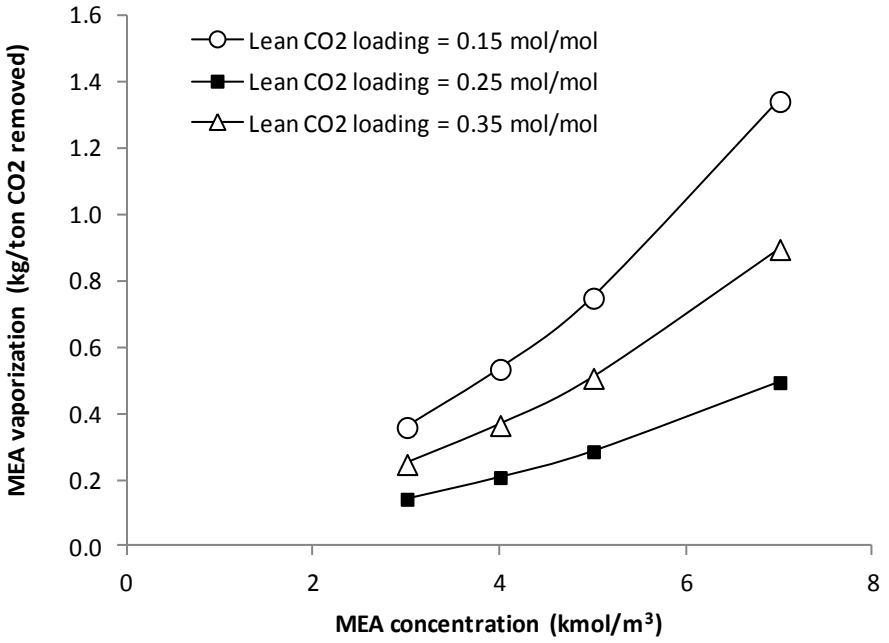

Figure 4.8: Effect of MEA concentration (90% capture efficiency; 40^{o}C feed gas; 0.40 mol/mol rich CO_2 loading; coal combustion)

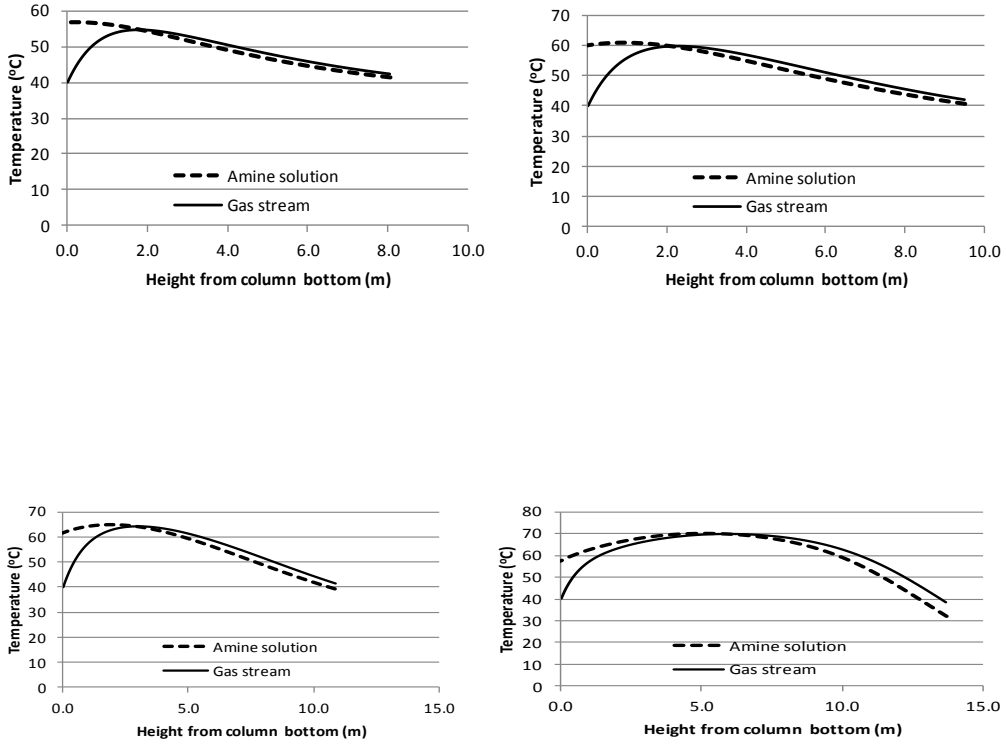

Figure 4.9: Temperature bulk along the absorption column at different MEA concentrations (90% capture efficiency; 40°C feed gas; 0.15 mol/mol lean CO_2 loading; 0.40 mol/mol rich CO_2 loading; coal combustion)

4.3.3 Effect of CO_2 capture efficiency

The percentage of CO_2 to be removed from the flue gas stream (referred to here as CO_2 capture efficiency) is an important factor that controls the economics of CO_2 capture. The capture efficiency also has a great impact on the amount of MEA vapour escaping from the absorber. As can be seen from Figures 4.10 - 4.11, higher capture efficiency offers lower MEA vapourization per ton of CO_2 capture. Reducing the capture efficiency from 90% to 50% causes the vaporization to increase by more than 70%, and almost 200% increase in vapour loss can be reached if the capture efficiency is reduced further to 30%. The exponential or progressing effect of reducing capture efficiency is primarily caused by the nonlinear increase in mass flow rate of exit gas stream leaving the absorber top. This is true when the CO_2 capture target is fixed (4.0 ton CO_2 /day in this study). More specifically, changing the capture efficiency from 90 % to 50% and then to 30% leads to an increase in exit gas flow from 672 kmol/day to 1283 and 2198 kmol/day, respectively.

4.3.4 Effect of feed gas temperature

It is commonly known that hot flue gas from the combustion must be cooled down to a specific temperature prior to entering the CO_2 absorber. In general, the cooling can be achieved by two techniques: i) direct contact cooling by scrubbing (referred to as scrubbing) and ii) indirect contact cooling through a heat exchanger (referred to as HEX in this study). At low cooling temperatures, both techniques can help reduce water content (or moisture content) in the flue gas as can be seen from Figure 4.12 (at 20 and 40^oC.However at the higher cooling temperature (such as 60^oC) use of direct scrubbing

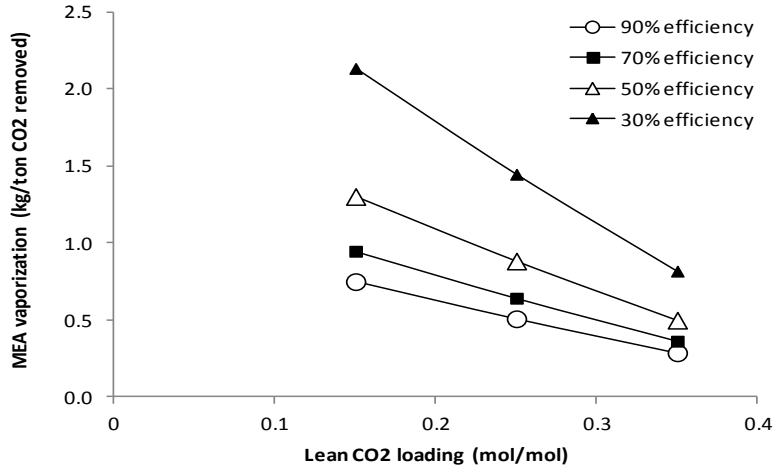

(a)

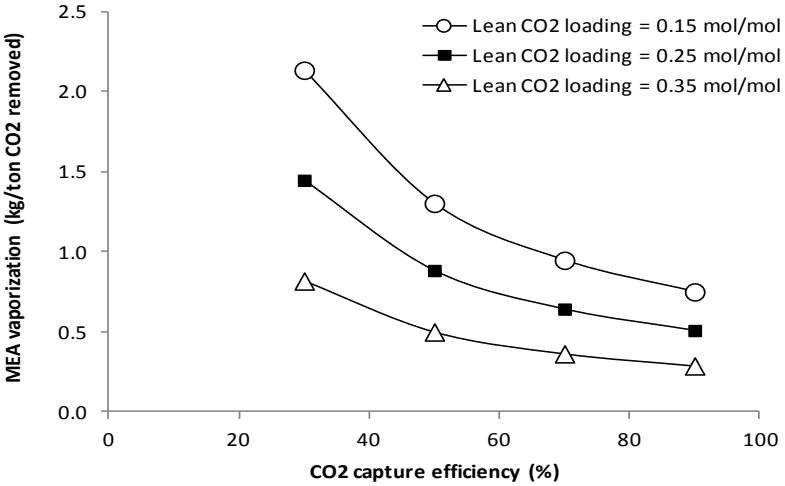

(b)

Figure 4.10: Effect of CO_2 capture efficiency (5.0 kmol/m^3 MEA solution; 40^oC feed gas; 0.40 mol/mol rich CO_2- loading; coal combustion)

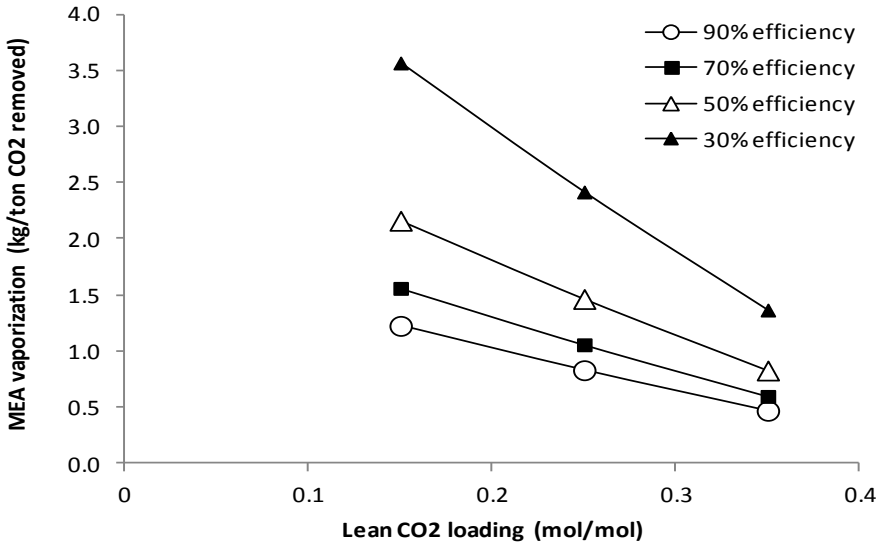

(a)

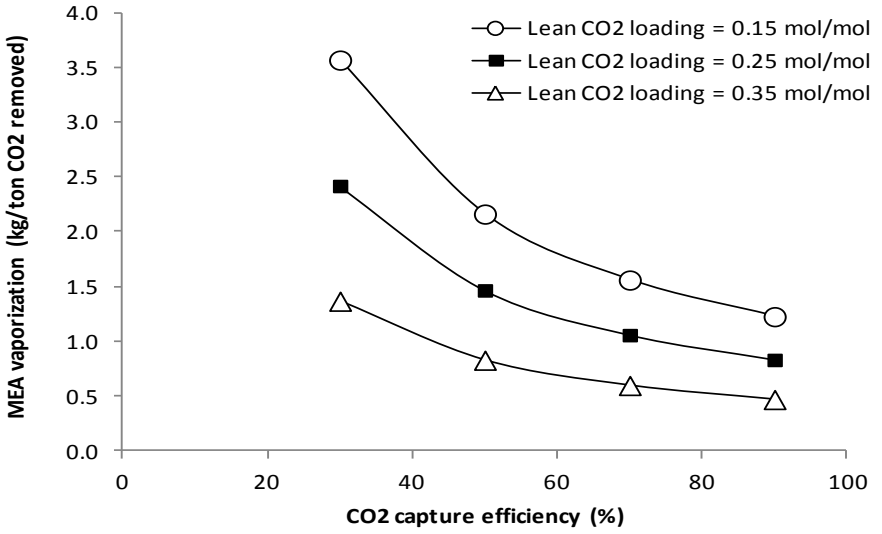

(b)

Figure 4.11: Effect of CO_2 capture efficiency (5.0 kmol/m^3 MEA solution; 40^oC feed gas; 0.40 mol/mol rich CO_2 loading; CH_4 combustion)

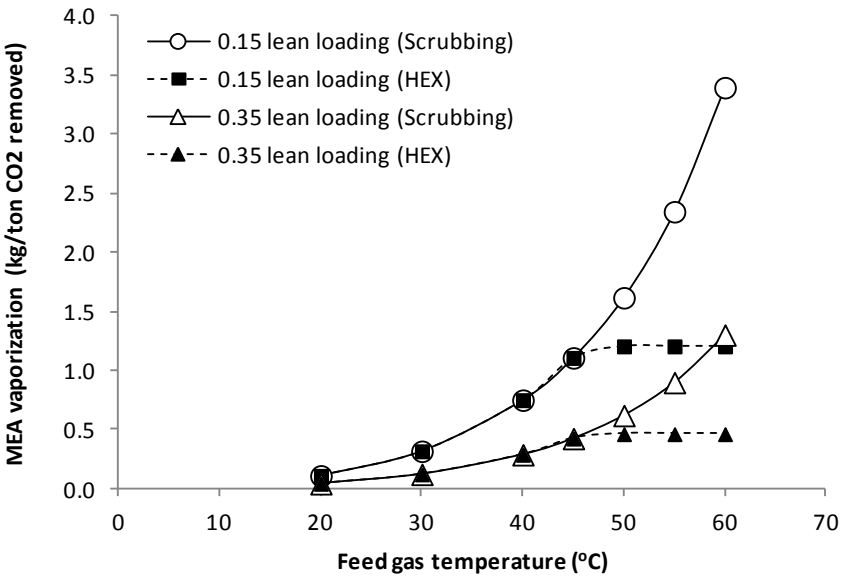

(a) Coal combustion

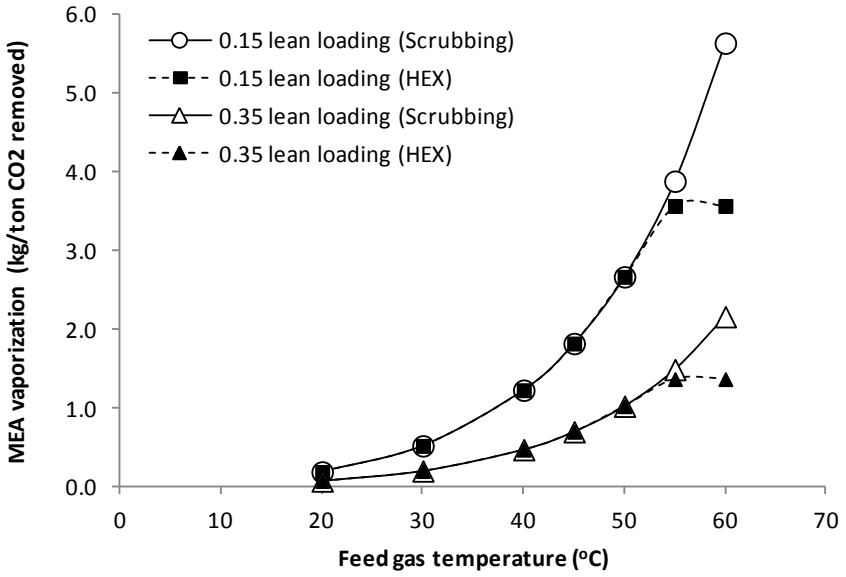

(b) CH_4 combustion

Figure 4.12: Effect of feed gas temperature with different lean CO_2 loadings and flue gas cooling techniques (5.0 kmol/m^3 MEA solution; 90% capture efficiency; 0.40 mol/mol rich CO_2 loading)

technique leads to an increase in moisture content beyond the value generated from combustion whereas the heat exchanger technique helps limit the moisture content to the combustion value. Because of the difference in flue gas quality (moisture content and other composition) caused by cooling techniques, the effect of feed gas temperature on amine vapourization will be discussed below in two different respects. In the case of scrubbing, an increase in feed gas temperature results in an exponential increase in MEA vapourization for the entire range of test temperatures. The increasing vapourization is a result of an increase in temperature of feed amine solution that keeps rising to maintain water balance around the absorber. In the case of HEX, the MEA vapourization increases with feed gas temperature until reaching a limit where the feed gas temperature has no impact. The limited vapourization is controlled by a fixed temperature of feed amine solution that is regulated by a constant moisture content of the feed gas.

4.3.5 Effect of fuel type

The type of fuel used during the combustion process also has an impact on MEA vapourization in the CO_2 capture process. This effect is derived from the difference in composition of produced flue gas. Combusting CH_4 produces flue gas with a CO_2 concentration of 7.24% while a flue gas with 12.88% CO_2 can be realized from coal combustion. From Figure 4.13, capturing CO_2 from coal-based flue gas (with higher CO_2 content) is subjected to lower amine vapourization compared to the capture from CH_4-based flue gas. The lower vapourization is a result of the lower amount of exit gas leaving the absorber top.

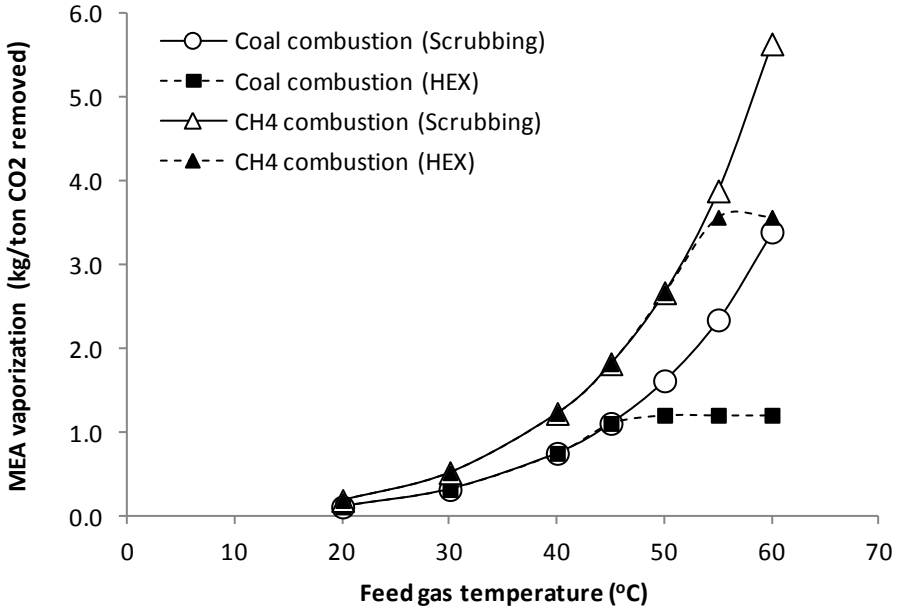

Figure 4.13: Effect of fuel type at different feed gas temperatures and flue gas cooling techniques (5.0 kmol/m^3 MEA solution; 90% capture efficiency; 0.15 mol/mol lean CO_2 loading; 0.40 mol/mol rich CO_2 loading)

4.3.6 Empirical correlations for MEA vapourization

As discussed above, the amount of MEA vapour escaping from the absorber column depends upon a number of process parameters. In this study, empirical correlations were developed from the simulation results presented earlier so as to make the data accessible to general users for estimating loss of MEA through vapourization. By using multiple regression technique, the MEA vapourization in a unit of kg/ton CO_2 captured (ψ_{MEA}) can be presented by Equation 4.7 as a function of temperature (K)

$$\psi_{MEA} = \phi_{\alpha}\, \phi_{\eta}\, \phi_{C}\, \phi_{fuel}\, \psi_{base} \tag{4.7}$$

Where lean CO_2 loading is (α in mol/mol), CO_2 capture efficiency is (η in %), MEA concentration is (C in kmol/m^3), fuel is(ϕ_{fuel}) type of fuel combusted (Dakota's lignite or CH_4). Here, ψ_{base} is the base value of vapourization, and ϕ_i is the correction factor for each individual parametric effect. These parameters can be written in mathematical form:

$$\psi_{base} = \begin{cases} 1.502 \times 10^{11}\, e^{\frac{-8.277}{T}} & for\ cooling\ by\ scrubbing \\ \min\left(0.8167\ ,\ 1.502 \times 10^{11}\, e^{\frac{-8.277}{T}}\right) & for\ HEX\ cooling\ of\ coal\ fired\ gas \\ \min\left(1.4427\ ,\ 1.502 \times 10^{11}\, e^{\frac{-8.277}{T}}\right) & for\ HEX\ cooling\ of\ CH4\ fired\ gas \end{cases} \tag{4.8}$$

$$\phi_{\alpha} = -4.5566\ (\alpha) + 2.1479 \tag{4.9}$$

$$\phi_{\eta} = 72.601\ \eta^{-0.95308} \tag{4.10}$$

$$\phi_{C} = 3.6632 \times 10^{-3} \left(\frac{1}{C+3.4}\right)^{-2.6372} \tag{4.11}$$

$$\phi_{fuel} = \begin{cases} 1.000 \text{ for North Dakota's lignite} \\ 1.677 \; for \; CH4 \; combustion \end{cases} \quad (4.12)$$

Note that the base amount of MEA vapourization (ψ_{base}) is affected by the way in which hot flue gas is cooled. A comparison between the simulated MEA vapourization and the corresponding values from empirical correlation is presented in form of a parity plot in Figure 4.14 with R^2 of 0.9987.

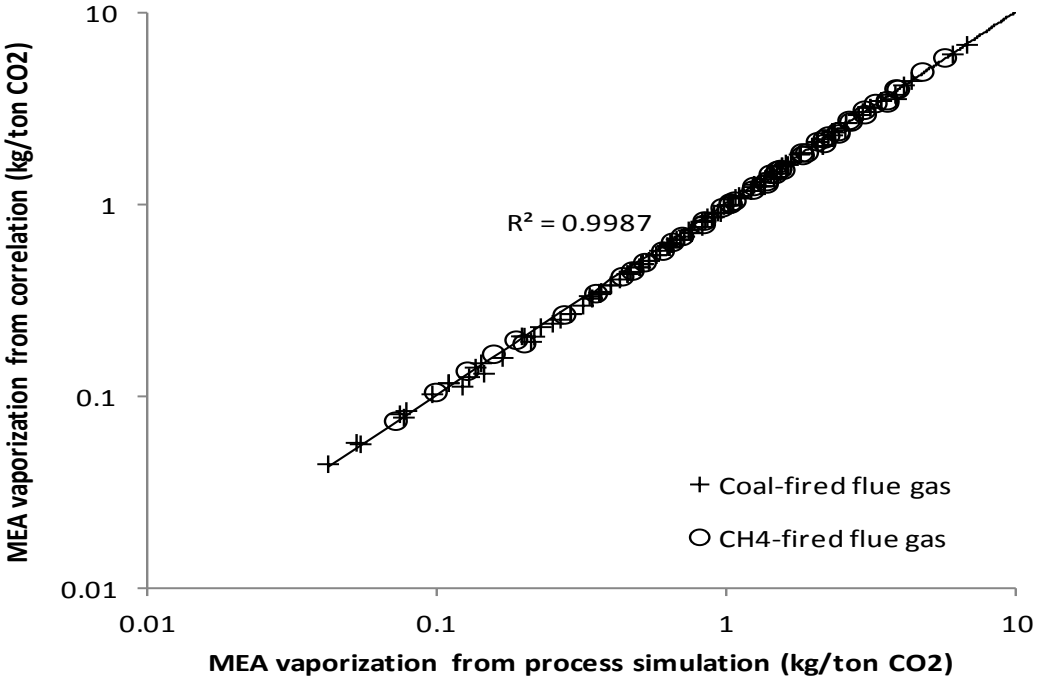

Figure 4.14: Parity plot

5. CONCLUSIONS AND FUTURE WORK

Amine vapourization loss was studied, and an empirical equation was developed to quantify the amine vapourization loss. Experimental vapour pressure data were generated and the activity coefficient was regressed using this data along with the available data in the literature. The experimental vapour pressure data obtained at a low range of concentration of MEA ranging from 1-7 kmol/m^3 showed high dispersion. This indicates that the concentration range chosen is very sensitive to the experimental conditions and requires high precision methods to generate vapour pressure data. The developed empirical equation was used to quantify amine loss. The quantified loss was further studied to analyse the effects of different parameters on the amine vapourization loss. Rich CO_2 loading has no impact on the MEA vapourization loss. Lean CO_2 loading, concentration of amine in the solution, feed gas temperature, and fuel types in the combustion process have certain degrees of impact on amine vaporization loss.

The following are recommendations for future work in this area of study:

1. Conducting further experiments for precision of vapour pressure data for MEA at different temperatures, pressures and concentrations;
2. Conducting experiments for binary and ternary amine solvents;
3. Parametric behaviour of CO_2 could be incorporated during the experimental study;
4. Thermodynamic modelling could be used to determine the accuracy of activity coefficients obtained from the experiments; and
5. Parametric effects on amine loss when cooling equipment has been installed on top of the absorber could be studied in terms of the efficiency in reducing the loss.

REFERENCES

Abdi, M., Meisen, A.(1999).A novel process for diethanolamine recovery from partially degraded solutions.1.Process description and phase equilibria of the DEA-BHEP-THEED-Hexadecane system, *Ind.Eng.Chem.Res.*38, 3096-3104.

Astarita, G., Savage, D.W., Bistro, A.(1983). *Gas Treating with Chemical Solvents*. New York: John Wiley & Sons.

Barreau, A., Mougin, P., Lefebvre, C., Luu Thi, M.Q., Rieu, J.(2007).Ternary Isobaric Vapour-Liquid Equilibria of Methanol+ *N*-Methyldiethanolamine+ Water and Methanol +2-Amino-2-methyl-1-propanol+Water Systems.*J. Chem. Eng. Data. 52*, 769-773.

Belabbaci, A., Razzouk, A., Mokbel,I., Jose,J.,Negadi,L.(2009).Isothermal Vapour-Liquid Equilibria of (Monoethanolamine + Water) and (4-Methylmorpholine + Water), binary systems at several Temperatures. *J. Chem. Eng. Data***.** 54, *2312*–2316.

Cai, Z., Xie, R., Wu, Z.(1996).Binary Isobaric Vapour-Liquid Equilibria of Ethanolamine's + Water. *J. Chem. Eng. Data***.** *41*, 1101-1103

Ciferno, P.J., Fout, E.T., Jones, P.A., Murphy, T.J.(2009).Capturing carbon from existing coal -fired power plants. *AIChe* ..

Chi, S., Rochelle, G. T.(2002).Oxidative degradation of monoethanolamine. *Ind. Eng. Chem. Res*. 41 (17), 4178–4186

Chowdhury, F.A., Higashii, T., Goto, K., Onoda, M., Kazama, S.(2011). Synthesis and selection of new amine absorbents for CO_2 capture, *1st Post Combustion Capture Conference*, May 2011.

Closmann, F., Nguyen, T., Rochelle, G. T.(2009). MDEA/Piperazine as a solvent for CO_2 capture. *Energy Procedia*. 1, 1351–1357.

Cummings, L.A., mecum, M.S.(2008).Increased profitability and improving environmental performance by maintaining amine solvent purity, Laurance Reid Gas Conditioning conference, 50th annual conference, Oklahoma.

Energy Information Administration (EIA).(2005).Emissions of Greenhouse Gases in the United States 2005.DOE / EIA- 0573.

Horstmann, S.,Mougin, P.,Lecomte, F.,Fischer, K.,Gmehling, J.(2002).Phase Equilibrium and Excess Enthalpy Data for the System Methanol + 2, 2- Diethanolamine + Water; *J. Chem. Eng. Data*, *47*, 1496-1501.

IPCC.1990. Policymaker's Summary of the Scientific Assessment of Climate Change, Report to IPCC from Working Group; Meteorological Office, Branknell, UK.

Kapteina, S.,Slowik, K.,Verevkin, P.S.,Heintz, A.(2005).Vapour Pressures and Vapourization Enthalpies of a Series of Ethanolamine's; *J. Chem. Eng. Data*, *50*, 398-402.

Kentish, S.,Hooper, B.,Stevens, G.,Perera, J.,Qiao, G.(2008).An overview of technologies for carbon capture.AIE National Conference.

Kim, I., Svendsen, F.H., Børresen, E. (2008).Ebulliometric Determination of Vapour-Liquid Equilibria for Pure Water, Monoethanolamine, *N*-Methyldiethanolamine, 3-(Methylamino)-propylamine, and their Binary and Ternary Solutions; *J. Chem. Eng. Data*, *53*, 2521–2531.

Klotz, M.I., Rosenberg, M.R, M.R.(1994).Chemical Thermodynamics: Basic Theory and methods, Wiley Publisher, 5th edition, Newyork.

Kohl, A. L., Nielsen, R. B. (1997).*Gas Purification*,(5thed.). Houston, Texas: Gulf PublishingCo.Krutka,H.M.,Sjostrom,S.,Bustard,C.J.,Durham,M.,Baldrey,K.,Stewart,R,(2008)Summary of Post-Combustion CO_2 capture Technologies for Existing coal-fired Power plants, ADA-ES,paper 808.

Lepaumier, H., Picq, D., Carrette, P. L.(2009).New amines for CO_2 capture. II. Oxidative degradation mechanism, *Ind. Eng. Chem. Res*., 48, 9068 – 9075.

McLees, A.J. (2006). Vapour liquid Equilibrium of monoethanolamine/Piperazine/water at 35-70^{o}C, Topical report, DOE Award no.DE-FC26-02NT41440.University of Texas.

Nath, A., Bendert, E.(1983).Isothermal Vapour-Liquid Equilibria of Binary and Ternary Mixtures Containing Alcohol, Alkanolamine, and Water with a New Static Device; *J. Chem. Eng. Data,* 28, 370-375.

Nguyen, T., Hilliard, M., Rochelle, T.G.,(2010), Amine volatility in CO_2 capture, *International Journal of greenhouse gas control* 4,707-715

Olson, D.James. (1989).Measurement of vapour-liquid equilibria by ebulliometry, Fluid Phase equilibria, 52,209-218.

Pappa, D.G.,Anastasi, C., C. Voutsas,C.E. (2006).Measurement and thermodynamic modeling of the phase equilibrium of aqueous 2-amino-2-methyl-1- propanol solutions; *Fluid Phase Equilibria* 243,193–197.

Park, B.S.,Lee, H.(1997).Vapour-liquid equilibria for the binary monoethanolamine+ water and monoethanolamine and ethanol systems; *Korean J. of Chem. Eng.*, 14(2), 146-148.

Park, J.S., Shin, Y.H.,Min, M.B.,Cho, A.,Lee, S.J.(2009).Vapour liquid equilibria of water+ monoethanolamine system; *Korean J. Chem. Eng*., 26(1), 189- 192.

Puxty,G.,Rowland,R.,Allport,A.,Yang,Q.,Bown,M.,Burns,R.,Maeder,M,Attalla,M,(2009) Carbon dioxide post combustion capture: A novel screening study of the carbon dioxide absorption performance of 76 amines, *Environ.Sci.Technol.*,43, 6427-6433.

Reid, E.C. (1990). Chemical Thermodynamics,McGraw Hill Inc., US.

Rogalski, M.,Malanowski, S.(1980).Ebulliometers modified for the accurate determination of vapour –liquid equilibrium, *Fluid phase equilibia*, 5,97-112.

Rubin, E., Coninck, M.L, (2005), Carbon dioxide Storage and Capture, IPCC Special Report

Shao, R.,Stangeland, A. (2009), Amines Used in CO_2 Capture- Health and environmental Impacts, Bellona Report.

Smith, E.B. (1973), Basic Chemical thermodynamics, Oxford Clarendon press

Stadler, H.P. (1989).Chemical Thermodynamics Revison and worked examples, Cambridge the Royal Society Chemistry 129p.

Stewart, E.J, Lanning, R.A. (1994). A systematic Technical Approach will identify and quantify loss into five categories, *Hydrocarbon Processing*, 67-84.

Tochigi, K., Akimoto, K., Ochi, K., Liu, F., Kawase, Y.(1999). Isothermal Vapor-Liquid Equilibria for Water + 2-Aminoethanol + Dimethyl Sulfoxide and Its Constituent Three Binary Systems; *J. Chem. Eng Data, 44*, 585-590.

Vrachnos,A., Kongtogeorgis,G., Voutsas,E.(2006).Thermodynamic modeling of acidic gas solubility in aqueous solutions of MEA,MDEA and MEA-MDEA blends,*Ind.Eng.Chem.*Res,45,5148-5154.

Voutsas, E., Athanassios Vrachnos, A., Magoulas, K.(2004).Measurement and thermodynamic modeling of the phase equilibrium of aqueous *N*-methyldiethanolamine solutions. *Fluid Phase Equilibria.*224, 193–197.

Xu, S., Qing, S., Zhen, Z., Zhang, C. (1991).Vapour pressure measurements of aqueous N-methyldiethanolamine solutions. *Fluid Phase Equilibria.* 67, 197-201.